

We are IntechOpen, the world's leading publisher of Open Access books Built by scientists, for scientists

6,900

Open access books available

186,000

International authors and editors

200M

Downloads

Our authors are among the

154

Countries delivered to

TOP 1%

most cited scientists

12.2%

Contributors from top 500 universities



WEB OF SCIENCE™

Selection of our books indexed in the Book Citation Index
in Web of Science™ Core Collection (BKCI)

Interested in publishing with us?
Contact book.department@intechopen.com

Numbers displayed above are based on latest data collected.
For more information visit www.intechopen.com



Determination of Elastic and Dissipative Energy Contributions to Martensitic Phase Transformation in Shape Memory Alloys

Dezso L. Beke, Lajos Daróczy and Tarek Y. Elrasasi

Additional information is available at the end of the chapter

<http://dx.doi.org/10.5772/51511>

1. Introduction

There is a long standing debate in the literature on shape memory alloys that while the contribution of the dissipative energy, D , to the austenite/martensite, A/M, (or reverse) transformation can be directly obtained from the experimental data (hysteresis loop, Differential Scanning Calorimeter, DSC, curves), the contributions from the elastic, E , and the chemical free energy, ΔG_c , can not be separated. The temperature dependence of $\Delta G_c = \Delta H - T\Delta S$ is described by $\Delta G_c = (T - T_0)\Delta S$, where $T_0 = \Delta S / \Delta H$ is the equilibrium transformation temperature (at which the chemical free energies of the two phases equals, i.e. $\Delta G_c = 0$) as well as ΔH and ΔS are the chemical enthalpy and entropy change of the phase transformation (they are negative for A to M transformation), respectively. The experimentally determined quantities (DSC or hysteresis curves) usually contain a combination of the chemical, elastic and dissipative terms in such a way [1] that always the sum of E and ΔG_c can be calculated and thus for their separation one would need the knowledge of ΔS and T_0 (see also below in details). While the direct determination of ΔS is possible (e.g. from the measured DSC curves) the determination of T_0 is rather difficult: it has been shown and experimentally illustrated that the simple expression proposed by Tong and Waynman [2]: $T_0 = (M_s + A_f) / 2$ (where M_s and A_f are the martensite start and austenite finish temperatures) can not be valid in general. Indeed Salzbrenner and Cohen [1] have been nicely illustrated that T_0 can be calculated from the above relation only in those cases when the elastic energy contributions to M_s and A_f can be neglected.

In this review we will summarize our model [3-8] for the thermal hysteresis loops, $\xi = \xi(T)$ (at constant other driving fields such as uniaxial stress, σ , magnetic field, B , or pressure, p) in terms of T_0 , and the derivatives $\partial \Delta S / \partial \xi = \Delta s$, $\partial E / \partial \xi = e$ and $\partial D / \partial \xi = d$, where ξ is the martensite

transformed (volume) fraction. (In the following quantities given by small letters denote the quantity belonging to unit volume fraction.) Similar relations for example for the strain, $\varepsilon(\sim\xi)$, versus σ (or e.g. magnetization, $\Delta m(\sim\xi)$, versus B) hysteresis loops can be derived, where instead of Δs , ε^{tr} (or Δm^{tr}) appears. Here ε^{tr} is the transformation strain (and Δm^{tr} is the change of magnetization) of phase transformation. The results obtained from the application of this model to our experimental data measured in single and polycrystalline CuAlNi alloys will be summarized too.

2. Description of the model

Our model is in fact a local equilibrium formalism and based on the thermoelastic balance (see e.g. [9,10] and [11]) offering a simple form of the elastic and dissipative energy contributions to the start and finish parameters [3-8]. The *total* change of the Gibbs free energy versus the transformed martensite fraction (if the hydrostatic pressure and the magnetic field are zero), for the A/M transformation (denoted by \downarrow), can be written in the form [3,8]:

$$\partial(\Delta G^\downarrow)/\partial\zeta = \partial(\Delta G_c^\downarrow + E + D)/\partial\zeta = \Delta g_c^\downarrow + e^\downarrow(\zeta) + d^\downarrow(\zeta) = 0. \quad (1)$$

where

$$\Delta g_c^\downarrow = \Delta u^\downarrow - T\Delta s^\downarrow - \sigma V \varepsilon^{tr\downarrow}, \quad (2)$$

with $\Delta s \stackrel{L}{=}_{SM-SA} (-\Delta s \uparrow < 0)$, and V is the molar volume. Similar expression holds for the M/A transformation (with upper index \uparrow):

$$\Delta g_c^\uparrow = \Delta u^\uparrow - T\Delta s^\uparrow - \sigma V \varepsilon^{tr\uparrow}. \quad (3)$$

The elastic energy accumulates as well as releases during the processes down and up just because the formation of different variants of the martensite phase usually is accompanied by a development of an elastic energy field (due to the transformation strain). It is usually supposed that $E_{el}^\downarrow = -E_{el}^\uparrow > 0$. The dissipative energy is always positive in both directions.

In thermoelastic transformations the elastic term plays a determining role. For example at a given under-cooling, when the elastic term will be equal to the chemical one, for the further growth of the martensite an additional under-cooling is required. Thus if the sample is further cooled the M phase will grow further, while if the sample is heated it will become smaller. Indeed in *thermoelastic* materials it was observed that once a particle formed and reached a certain size its growth was stopped and increased or decreased as the temperature was decreased or raised. This is the *thermoelastic behaviour* (the thermal and elastic terms are balanced).

In principle, one more additional term, proportional to the entropy production, should be considered, but it can be supposed [12] that for thermoelastic transformations all the energy losses are mechanical works, which are dissipated without entropy production, i.e. the

dissipation is mainly energy relaxation in the form of elastic waves. Indeed acoustic waves were detected as acoustic emissions during the transformation. Thus in the following the term proportional to the entropy production will be neglected. Furthermore, usually there is one more additional term in ΔG : this is the nucleation energy related to the formation of the interfaces between the nucleus of the new phase and the parent material. However, since this term, similarly to the dissipative energy, is positive in both directions and thus it is difficult to separate from D , it can be considered to be included in the dissipative term.

According to the definitions of the equilibrium transformation temperature and stress

$$T_o(0) = \Delta u^\downarrow / \Delta s^\downarrow = \Delta u^\uparrow / \Delta s^\uparrow, \quad (4)$$

$$\sigma_o(0) = \Delta u^\downarrow / V \varepsilon^{tr\downarrow}(T=0) = \Delta u^\uparrow / V \varepsilon^{tr\uparrow}(T=0), \quad (5)$$

respectively.

Δg_c^\downarrow , if the external hydrostatic pressure, p , and magnetic field, B , are also not zero, can have the general form as:

$$\Delta g_c^\downarrow = \Delta u^\downarrow - T \Delta s^\downarrow - s V \varepsilon^{tr\downarrow} + p \Delta v^\downarrow - B \Delta m^{tr\downarrow}, \quad (6)$$

where Δv^\downarrow is the volume change of the phase transformation.

It is plausible to assume that Δu^\downarrow , Δs^\downarrow and Δv^\downarrow are independent of ξ , i.e. ΔU , ΔV and ΔS linearly depends on the transformed fraction. On the other hand the terms containing ε^{tr} and Δm^{tr} in general have tensor character and, as a consequence, even if one considers uniaxial loading condition, leading to scalar terms in (2), the field dependence of these quantities is related to the change of the variant/domain distribution in the martensite phase with increasing field parameters. Thus at zero σ (or B) values thermally oriented multi-variant martensite structure (or multi-variant magnetic domain structure) forms in thermal hysteresis, while at high enough values of σ (or B) a well oriented array i.e. a single variant (or single domain structure) develops. For the description of this, the volume fraction of the stress induced (single) variant martensite structure, η , can be introduced [8]: $\eta = V_{M\sigma} / V_M$, ($V_M = V_{MT} + V_{M\sigma}$ and $\xi = V_M / V$, with $V = V_M + V_A$, where V_M and V_A are the volume of the martensite and austenite phases, respectively and V_{MT} and $V_{M\sigma}$ denotes the volume of the thermally as well as the stress induced martensite variants, respectively). The concept of introduction of this parameter was based e.g. on works of [11, 13-15]. Accordingly, e.g. ε^{tr} is maximal for $\eta=1$, and $\varepsilon^{tr\uparrow}(\eta=1) = \varepsilon^{tr\uparrow}_{max}$ in single crystalline sample, while it can be close to zero for $\eta=0$. In the following only the case of simultaneous action of temperature and uniaxial stress will be treated (extension to more general cases is very plausible).

Thus, in (2) and (3) ε^{tr} depends on η . Since η depends on T and σ , $\varepsilon^{tr\uparrow}$ can also depend on T or σ at fixed σ or T , respectively.

From (1) with (2):

$$\Delta u^\downarrow - T\Delta s^\downarrow - \sigma V \varepsilon^{tr\downarrow} + e^\downarrow + d^\downarrow = 0. \quad (7)$$

For fixed σ parameter(s) from (6) and using also (4) for Δu (for both up and down processes);

$$T^\downarrow(\zeta) = T_o(0) - \sigma V \varepsilon^{tr\downarrow}(\sigma) / \Delta s^\downarrow + (e^\downarrow(\zeta) + d^\downarrow(\zeta)) / \Delta s^\downarrow = T_o(\sigma) + (e^\downarrow(\zeta) + d^\downarrow(\zeta)) / \Delta s^\downarrow \quad (a)$$

$$T^\uparrow(\zeta) = T_o(0) - \sigma V \varepsilon^{tr\uparrow}(\sigma) / \Delta s^\uparrow + (e^\uparrow(\zeta) + d^\uparrow(\zeta)) / \Delta s^\uparrow = T_o(\sigma) + (e^\uparrow(\zeta) + d^\uparrow(\zeta)) / \Delta s^\uparrow. \quad (b)$$

Here $T_o(\sigma)$ is the same for both directions, since $\varepsilon^{tr\downarrow} / \Delta s^\downarrow = \varepsilon^{tr\uparrow} / \Delta s^\uparrow$ ($\varepsilon^{tr\downarrow} = -\varepsilon^{tr\uparrow}$, as well as $\Delta s^\downarrow = -\Delta s^\uparrow$ and in our case $\varepsilon^{tr\downarrow} > 0$ and $\Delta s^\downarrow < 0$).

The inverses of (8a) and (8b), i.e. the $\xi(T^\downarrow)$ and $\xi(T^\uparrow)$ functions, are the down and up branches of the thermal hysteresis loops at fixed σ . Furthermore, the temperature at which (8a) is equal to zero at $\xi=0$ as well as $\xi=1$ is the martensite start (M_s) and finish (M_f) temperature, respectively. Similar definitions hold for the austenite start and finish temperatures, A_s and A_f , respectively (see eq. (8b)). Figure 1 illustrates the shape of the hysteresis curves for the following schematic cases: a) both $d(\xi)$ and $e(\xi)$ are zero; b) $e(\xi)=0$ and $d(\xi) \neq 0$, but $d(\xi)$ is constant; c) $d(\xi)$ is constant and $e(\xi)$ linearly depends on ξ . It can be seen that in a) the transformation takes place at T_o , in both directions, in b) there is already a hysteresis, but the $\xi(T^\downarrow)$ and $\xi(T^\uparrow)$ branches are vertical. For the case of c) the hysteresis curve is tilted, reflecting the ξ dependence of e .

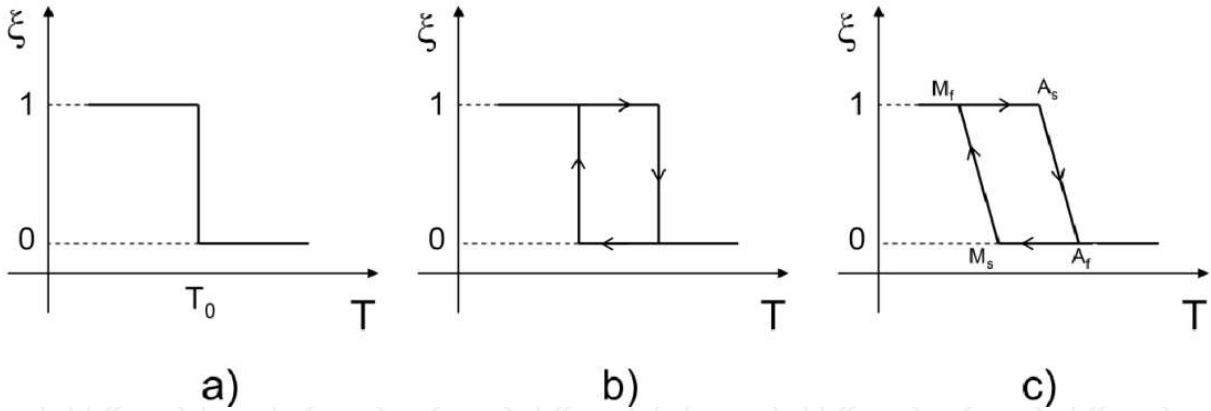


Figure 1. Thermal hysteresis loops schematically, see also the text.

Similarly as above but for fixed temperature(s), and now inserting Δu from (5),

$$\sigma^\downarrow(\zeta) = \sigma_o(0) V \varepsilon^{tr\downarrow}(\sigma_o) / V \varepsilon^{tr\downarrow}(T) - T \Delta s^\downarrow / V \varepsilon^{tr\downarrow}(T) + (e^\downarrow(\zeta) + d^\downarrow(\zeta)) / V \varepsilon^{tr\downarrow}(T) = \quad (a)$$

$$\sigma_o(T) + (e^\downarrow(\zeta) + d^\downarrow(\zeta)) / V \varepsilon^{tr\downarrow}(T) \quad (9)$$

$$\sigma^\uparrow(\zeta) = \sigma_o(0) V \varepsilon^{tr\uparrow}(\sigma_o) / V \varepsilon^{tr\uparrow}(T) - T \Delta s^\uparrow / V \varepsilon^{tr\uparrow}(T) + (e^\uparrow(\zeta) + d^\uparrow(\zeta)) / V \varepsilon^{tr\uparrow}(T) = \quad (b)$$

$$\sigma_o(T) + (e^\uparrow(\zeta) + d^\uparrow(\zeta)) / V \varepsilon^{tr\uparrow}(T).$$

Here again $\sigma_o(T)$ is the same taking also into account that $\varepsilon^{tr\uparrow}(\sigma_o) / \varepsilon^{tr\uparrow}(T) = \varepsilon^{tr\downarrow}(\sigma_o) / V \varepsilon^{tr\downarrow}(T)$, because the magnitude of the transformation strain is the same for the up and down branches of the loop at fixed T .

It can be seen from relations (8) and (9) that, in the case of the simultaneous action of temperature and uniaxial stress only, the stress dependence of the equilibrium transformation temperature, as well as the temperature dependence of the equilibrium transformation stress, introducing the notation $\Delta s = \Delta s^\downarrow = -\Delta s^\uparrow (< 0)$, can be given as

$$T_o(\sigma) = T_o(0) + \sigma V \varepsilon^{tr}(\sigma) / (-\Delta s), \quad (10)$$

and

$$\sigma_o(T) = \sigma_o(0) \varepsilon^{tr}(\sigma_o) / \varepsilon^{tr}(T) - T \Delta s / V \varepsilon^{tr}(T) = [T_o(0) - T] \Delta s / V \varepsilon^{tr}(T), \quad (11)$$

respectively. It can be seen that (10) and (11) are the well known Clausius-Clapeyron relations and they are linear only if $\varepsilon^{tr}(\sigma)$ as well as $\varepsilon^{tr}(T)$ are constant. It will be illustrated below that in most of the cases this is not fulfilled.

Now taking the assumptions usual in the treatment of thermoelastic transformations, i.e. assuming that the magnitudes of elastic and dissipative energies and their derivatives are the same in both A/M and M/A transformations; $e(\xi) = e^\downarrow(\xi) = -e^\uparrow(\xi)$ as well as $d(\xi) = d^\downarrow(\xi) = d^\uparrow(\xi)$, (8a) and (8b) can be rewritten as

$$\begin{aligned} T^\downarrow(\zeta) &= T_o(\sigma) - [e(\zeta) + d(\zeta)] / (-\Delta s) \quad (a) \\ T^\uparrow(\zeta) &= T_o(\sigma) + [d(\zeta) - e(\zeta)] / (-\Delta s). \quad (b) \end{aligned} \quad (12)$$

Thus

$$T^\uparrow(\zeta) - T^\downarrow(\zeta) = 2d(\zeta) / (-\Delta s) \quad (13)$$

and

$$T^\uparrow(\zeta) + T^\downarrow(\zeta) = 2T_o(\sigma) - 2e(\zeta) / (-\Delta s) \quad (14)$$

Furthermore, for the branches of the $\xi(\sigma)$ hysteresis loops

$$\begin{aligned} \sigma^\downarrow(\zeta) &= \sigma_o(T) + [e(\zeta) + d(\zeta)] / V \varepsilon^{tr}(T) \quad (a) \\ \text{and} \\ \sigma^\uparrow(\zeta) &= \sigma_o(T) - [d(\zeta) - e(\zeta)] / V \varepsilon^{tr}(T). \quad (b) \end{aligned} \quad (15)$$

Thus

$$\sigma^\downarrow(\zeta) - \sigma^\uparrow(\zeta) = 2d(\zeta) / V \varepsilon^{tr}(T) \quad (16)$$

and

$$\sigma^\downarrow(\zeta) + \sigma^\uparrow(\zeta) = 2\sigma_o(T) + 2e(\zeta) / V \varepsilon^{tr}(T). \quad (17)$$

It can be seen from eqs. (12)-(17) that, as it was mentioned in the introduction, while the dissipative term can be directly calculated from the hysteretic loops, the elastic and chemical terms appear in sums on the right hand sides of (14) and (17). It is worth noting that the integrals of (13) as well as (16), as it is expected, are nothing else than the area of the thermal and mechanical hysteresis loops, respectively.

Nevertheless, relations (10)-(17) allow the determination of the dissipative and elastic energy contributions as the function of ξ at different fixed values of σ as well as T from the thermal and stress induced hysteresis loops, respectively. Thus even the σ and T dependence of E and D can be calculated by integrating the $e(\xi)$ and $d(\xi)$ functions between $\xi=0$ and $\xi=1$. It should be noted that the elastic energy contribution can be determined only exclusive the term $T_o(0)$ if its value is not known. The values of Δs can be obtained from DSC measurements (see also below) and the $\varepsilon^{\text{tr}}(T)$ and $\varepsilon^{\text{tr}}(\sigma)$ values can be read out from the $\varepsilon(\sigma)$ and $\varepsilon(T)$ hysteresis loops, respectively. Thus e.g. the stress or temperature dependence of the elastic energy contribution can be determined, since $T_o(0)$ appears only in the intercept of the $e(\sigma)$ and $e(T)$ or $E(\sigma)$ and $E(T)$ functions.

From relations (12) and (15) expressions for the start and finish temperatures as well as stresses can be simply obtained at $\xi=0$ and at $\xi=1$:

$$\begin{aligned} M_s(\sigma) &= T_o(\sigma) - [d_o + e_o] / [-\Delta s] \\ M_f(\sigma) &= T_o(\sigma) - [d_1 + e_1] / [-\Delta s] \\ A_f(\sigma) &= T_o(\sigma) + [d_o - e_o] / [-\Delta s] \\ A_s(\sigma) &= T_o(\sigma) + [d_1 - e_1] / [-\Delta s] \end{aligned} \quad (18)$$

and

$$\begin{aligned} \sigma_{Ms}(T) &= \sigma_o(T) - [d_o + e_o] / [-V\varepsilon^{\text{tr}}] \\ \sigma_{Mf}(T) &= \sigma_o(T) - [d_1 + e_1] / [-V\varepsilon^{\text{tr}}] \\ \sigma_{Af}(T) &= \sigma_o(T) + [d_o - e_o] / [-V\varepsilon^{\text{tr}}] \\ \sigma_{As}(T) &= \sigma_o(T) + [d_1 - e_1] / [-V\varepsilon^{\text{tr}}]. \end{aligned} \quad (19)$$

Here in principle the d_o, d_1, e_o and e_1 can also be σ or T -dependent: in this case e.g. the stress dependence of the start and finish temperatures can be different from the stress dependence of T_o . It can be seen from relations (18) that the simple expression proposed by Tong and Waynman [2] for T_o as $T_o = (M_s + A_f)/2$ can be valid only if e_o is zero. Indeed Salzbrenner and Cohen [1] illustrated that T_o can be calculated only in those cases when the elastic energy contributions to M_s and A_f can be neglected. In their paper the phase transformation was driven by a slowly moving temperature gradient in a single crystalline sample, which resulted in slow motion of only one interface across the specimen (single-interface transformation). This way the elastic energy could easily relax by the formation of the surface

relief at the moving (single) phase-boundary. In general experiments for the determination of hysteresis loops, where typically many interfaces move simultaneously and the elastic fields of the different nuclei overlap, this separation is not possible. However, as we have shown in [5], and as it will be illustrated below, in single crystalline samples under relatively slow heating (cooling) rates, from the analysis of the different shapes of the hysteresis curves at low and high stress levels T_0 can be determined experimentally as the function of σ .

Finally it is worth summarizing what kind of information can be obtained from the analysis of results obtained by differential scanning calorimeter, DSC. The heats of transformation measurable during both transitions are given by

$$Q^\downarrow = \int [\Delta u_c^\downarrow + e(\zeta) + d(\zeta)] d\zeta \quad (20)$$

and

$$Q^\uparrow = \int [-\Delta u_c^\downarrow - e(\zeta) + d(\zeta)] d\zeta. \quad (21)$$

It is worth noting that the heat measured is negative if the system evolves it: thus e.g. the first term in (20) has a correct sign, because it is negative ($\Delta u_c^\downarrow < 0$). Similarly the dissipative and elastic terms should be positive for cooling (the system absorbs these energies): indeed $e(\xi), d(\xi) > 0$, while for heating $e(\xi)^\downarrow = -e(\xi)^\uparrow = e(\xi)$ and $d(\xi)^\downarrow = d(\xi)^\uparrow = d(\xi)$.

Now, using the notations $\int \Delta u_c^\downarrow = \Delta U_c (< 0)$, $\int d(\xi) d\xi = D (> 0)$, $\int e(\xi) d\xi = E (> 0)$

$$Q^\downarrow = \Delta U_c + E + D \quad (22)$$

and

$$Q^\uparrow = -\Delta U_c - E + D. \quad (23)$$

(In obtaining (22) and (23) it was used that Δu_c^\downarrow is independent of ξ .) Consequently

$$Q^\uparrow - Q^\downarrow = -2\Delta U_c + 2E \quad (24)$$

and

$$Q^\uparrow + Q^\downarrow = 2D. \quad (25)$$

It is important to keep in mind that the last equations are strictly valid only if after a cycle the system has come back to the same thermodynamic state, i.e. *it does not evolve from cycle to cycle*. Furthermore, it can be shown [12] that these are only valid if the heat capacities of the two phases are equal to each other: $c_A \cong c_M$, which was the case in our samples (see also below). The DSC curves also offer the determination of Δs . Indeed from the Q versus T curves, taking the integrals of the $1/T$ curves by Q^\downarrow or Q^\uparrow between M_s and M_f , as well as between A_s and A_f , respectively, one gets the Δs^\downarrow as well as Δs^\uparrow values. If, again, the $c_A \cong c_M$ condition fulfils, then $\Delta s^\downarrow \cong \Delta s^\uparrow$ [12].

Finally, it is possible, by using the DSC curve [I6], to obtain the volume fraction of the martensite, ξ , as a function of temperature (both for cooling and heating) as the ratio of the partial and full area of the corresponding curve (A_{Ms-T} and A_{Ms-Mf} , respectively: see also Figure 2):

$$\xi(T^\downarrow) = \frac{A_{Ms-T}}{A_{Ms-Mf}} = \frac{\int_{M_s}^T \frac{dQ^\downarrow}{T}}{\int_{M_s}^{M_f} \frac{dQ^\downarrow}{T}}. \quad (26)$$

Similar relation holds for the $\xi(T^\uparrow)$ curve (obviously in this case the above integrals run between A_s and T as well as A_s and A_f , respectively). The denominator is just the entropy of this transformation.

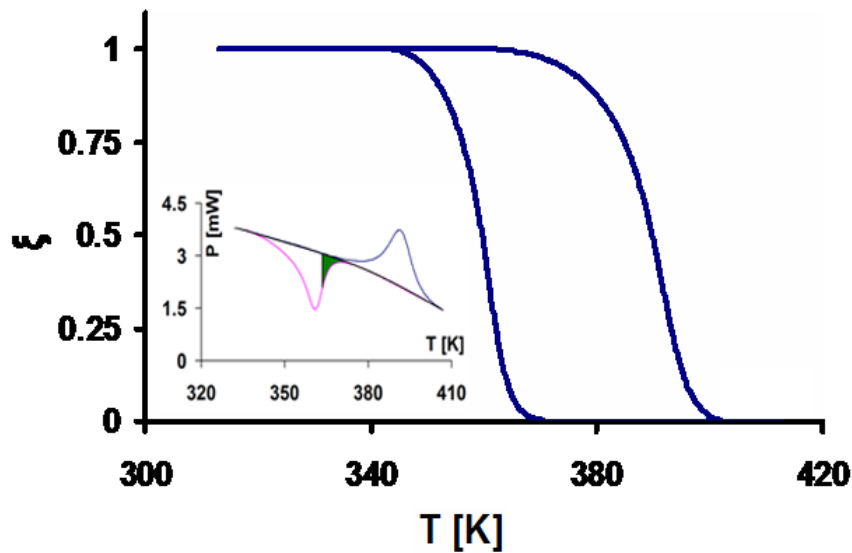


Figure 2. DSC curve measured at zero stress (a) and the $\xi(T)$ hysteresis curve (b): the dashed area (on the cooling down curve in a)) can be transformed to the nominator of equation (26); see also the text and [17].

3. Analysis of experimental data

3.1. Stress and temperature dependence of the transformation strain

As it was mentioned in the previous section it is generally expected that the transformation strain depends on the martensite variant structure developed. Since for thermal hysteresis loops this structure can vary from the randomly oriented structure to a well oriented single variant structure with increasing uniaxial stress, ε^r should increase with σ . Figure 3b shows this function for single crystalline CuAl(11.5wt%)Ni(5.0wt%) alloy (the applied stress was parallel to the [110] direction), as determined from the saturation values of the ε - T loops shown in Figure 3a [18]. In this alloy (i.e. at this composition) the β (austenite) to β' (18R, martensite) transformation takes place. Figure 4a shows the temperature dependence of ε^r , in the same alloy, as determined from the σ - ε loops shown in Figure 4b [18]. It can be seen that ε^r increases with increasing temperature

and saturates at the same maximal value which is obtained from the ε^{tr} versus σ plot and is approximately equal to the maximal possible transformation strain, ε^{tr}_{max} , corresponding to the estimated value for the case when a single crystal fully transforms to the most preferably oriented martensite [19].

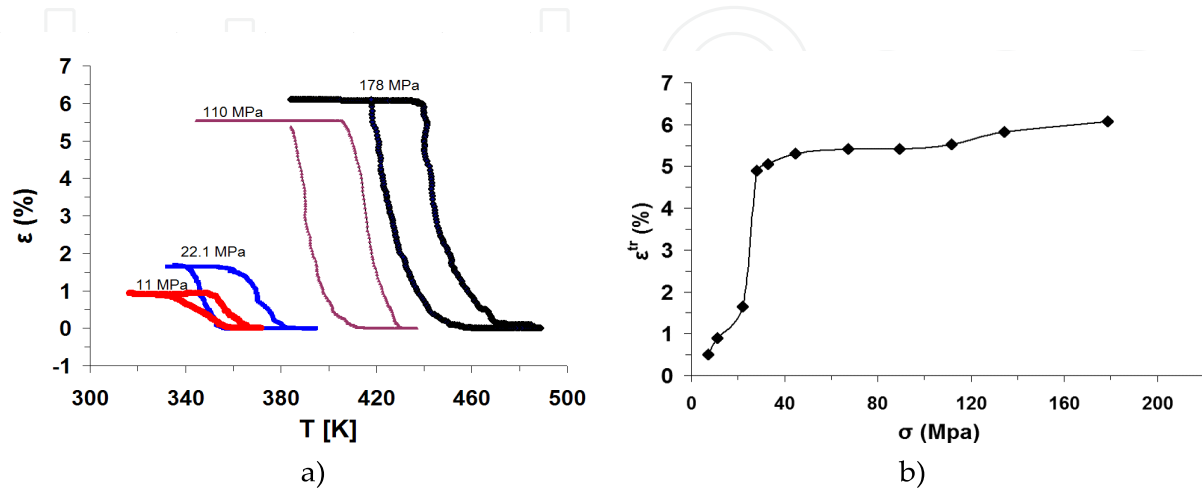


Figure 3. a) Thermal hysteresis loops (ε versus T curves) at four different uniaxial stress levels, b) Transformation strain as function of stress (ε^{tr} is the maximal of value of ε in a) for β/β' transformation in single crystalline CuAl(11.5wt%)Ni(5.0wt%) alloy [18].

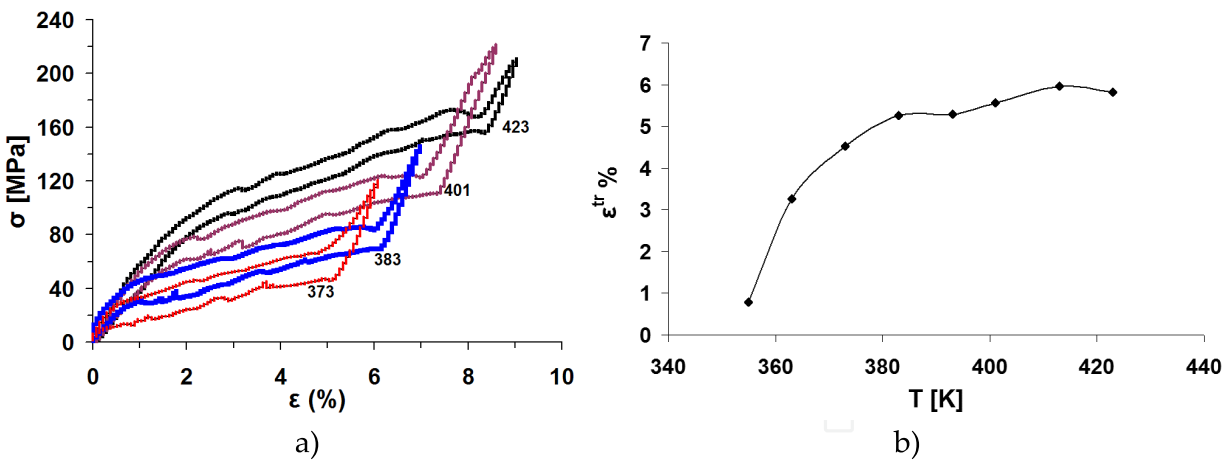


Figure 4. a) σ versus ε curves at four different temperatures, b) transformation strain as the function of the temperature (read out from curves like shown in a) in single crystalline CuAl(11.5wt%)Ni(5.0wt%) alloy for β/β' transformation [18].

Figure 5 shows the stress dependence of the transformation strain for the β to orthorhombic $\gamma(2H)$ phase transformation obtained in CuAl(17.9w%)Ni(2.6 w%) single crystalline alloy in [5]. It can be seen that it has S shape dependence with a saturation value of 0.075. It is interesting that in this case ε^{tr} has a finite (remanent) value even at $\sigma=0$.

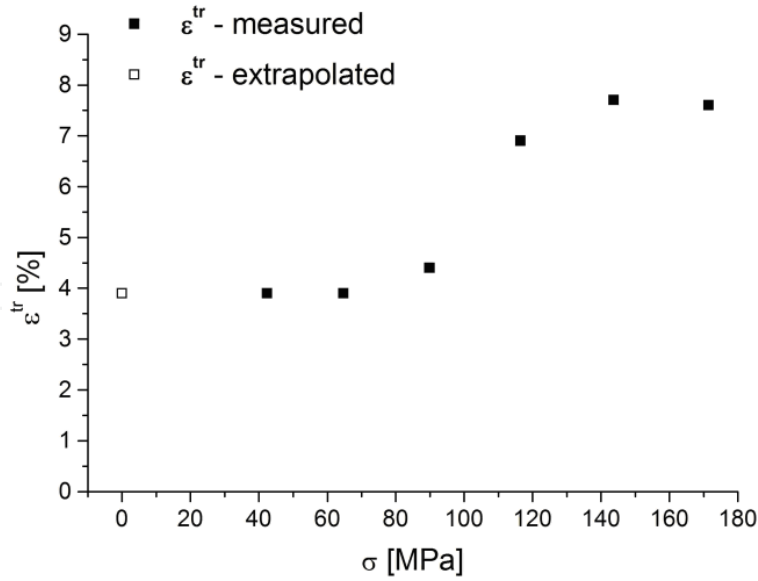


Figure 5. Stress dependence of ε^{tr} in CuAl(17.9w%)Ni(2.6 w%) single crystalline alloy for β/γ transformation [5].

As it was analyzed in detail in [19], from the above curves the η dependence of ε^{tr} can be constructed using the relation introduced in [8]:

$$\varepsilon^{tr} = \varepsilon_T + (\varepsilon_s - \varepsilon_T)\eta, \quad (27)$$

where ε_T and ε_s are the transformation strains when fully thermally induced multi variant structure forms ($\eta=0$), as well as when the martensite consists of a fully ordered array of stress preferred variants (single variant state, $\eta=1$), respectively. Thus ε^{tr} can be very small or even close to zero for the formation of the thermally induced (randomly oriented) martensite variants (usually there is a small resultant (remanent) strain in single crystalline samples). On the other hand during the formation of stress induced martensite a single variant structure can form ($\eta=1$) i.e. $\varepsilon^{tr}=\varepsilon_{max}^{tr}=\varepsilon_s$. On the basis of the experimental curves shown in Figure 3b, 4b and 5 as well as of relation (27) it can be concluded that a fully ordered single variant martensite structure develops above 140 MPa for the β/γ phase transformation, while for the β/β' transformation η is about 80% already for 28 MPa and then gradually increases up to 100% in the 40 - 178 MPa interval. As regards the temperature dependence of η , it can be seen from Figure 4a that (according to eq. (27) $\varepsilon_T \approx 0$ and $\varepsilon_s = 0.061$) η monotonously increases from about 10% up to 100% between 350 and 430 K.

Thus it can be concluded that the transformation strain depends both on the uniaxial stress and on the temperature and this dependence is related to the change of the martensite variant distribution with increasing field parameters. Then it is plausible to expect that the Clausius-Clapeyron type relations (see eqs. (10) and (11)) should also be non linear. Furthermore, the elastic and dissipative energy contributions should also be influenced by the martensite variant distribution. These points will be discussed in detail in the following sections.

3.2. Stress dependence of the equilibrium transformation temperature

In reference [5] we have investigated the thermal hysteresis loops in CuAl(17.9w%)Ni(2.6 w%) single crystalline alloy at different uniaxial stresses (applied along the $[110]_A$ axis). Very interesting shapes were obtained (see Figure 6): the ε - T loops had vertical parts, indicating that at these parts there were no elastic energy contributions (see also Figure 1c), allowing the determination of T_0 from the start and finish temperatures (see also eqs. (18)) either using the Tong-Waymann formula, $T_0=(M_s+A_f)/2$, (see the curve at 171.5 MPa in Figure 6) or $T_0=(M_s+A_s)/2$ (see e.g. the curve at 42.4 MPa in Figure 6). Thus it was possible (using also relation (10) and the value of the entropy, $\Delta s=-1.169 \cdot 10^5 \text{ J/Km}^3$, determined also in [5] and the stress dependence of ε^{tr} shown in Figure 5) to determine the stress dependence of T_0 as it is shown in Figure 7. It can be seen that this is indeed not a linear function.

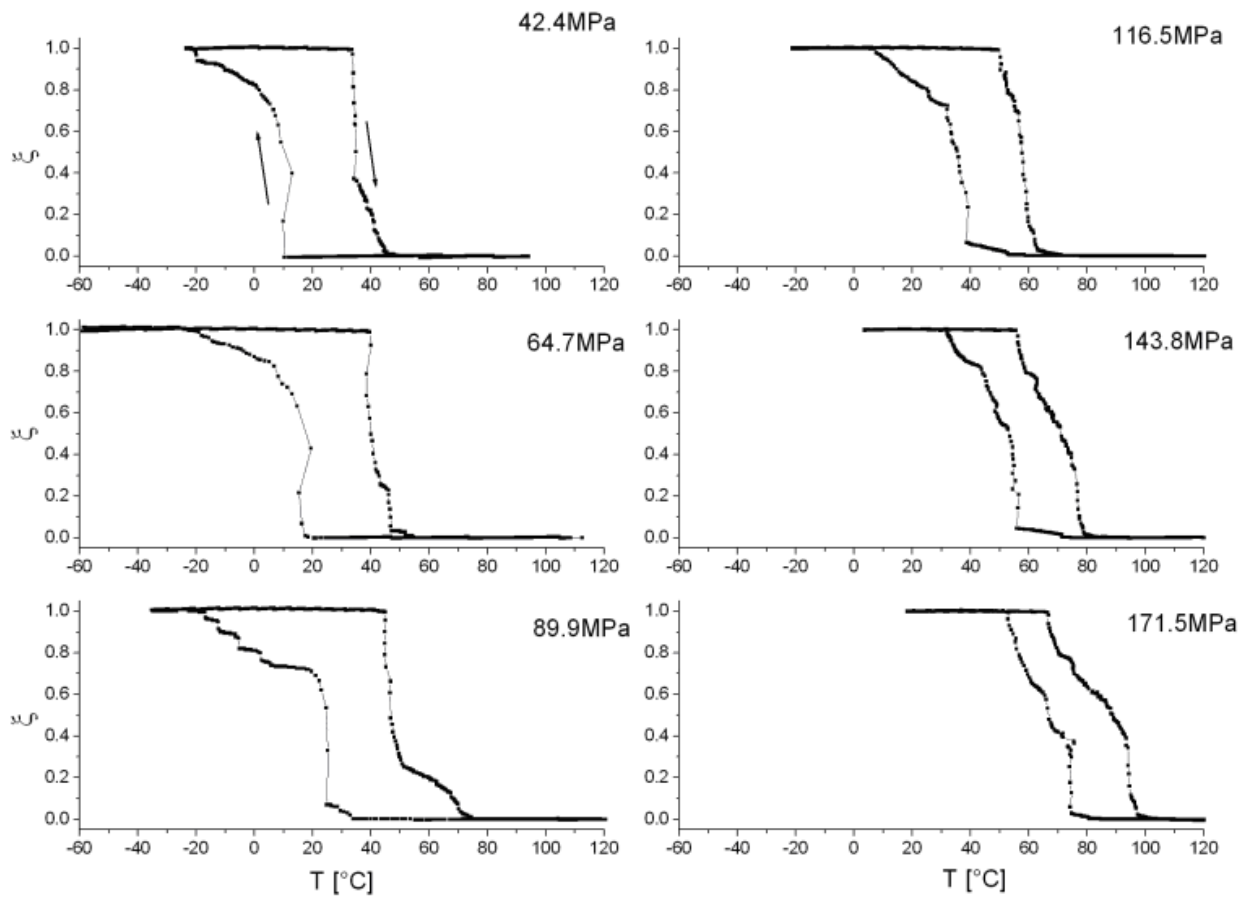


Figure 6. Thermal hysteresis loops at different stress levels in CuAl(17.9w%)Ni(2.6 w%) single crystalline alloy [5].

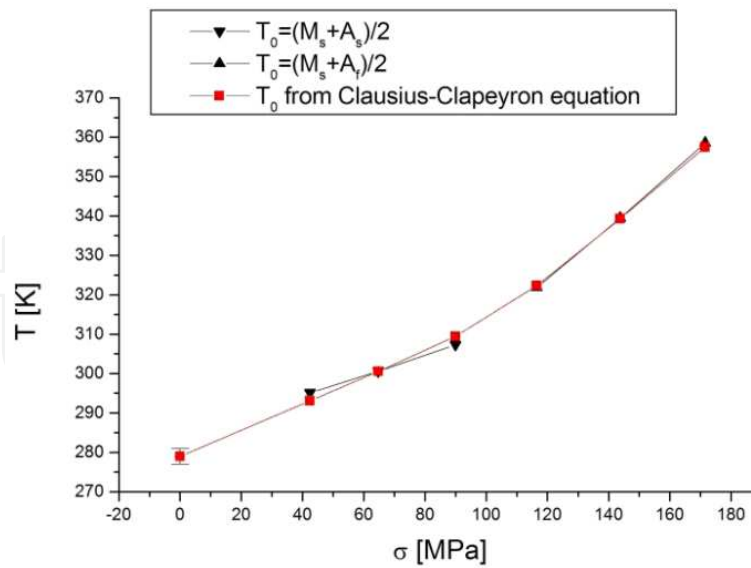


Figure 7. Stress dependence of T_0 in in CuAl(17.9wt%)Ni(2.6wt%) single crystalline alloy [5].

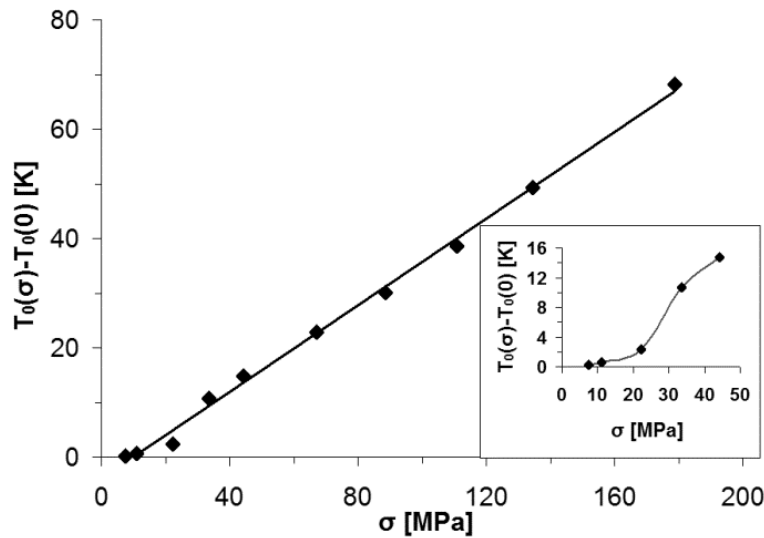


Figure 8. Stress dependence of T_0 in single crystalline CuAl(11.5wt%)Ni(5.0wt%) alloy [18].

Figure 8 shows the stress dependence of T_0 for the β/β transformation. In this case the determination of absolute values of T_0 was not possible, but the $T_0(\sigma) - T_0(0)$ difference could be calculated using the measured Δs value and the $\epsilon^{tr}(\sigma)$ curve (Figure 3b). It can be seen that this function can be approximated by a straight line in the entire stress interval. But, as it is illustrated in the insert of this figure, if we plot this function only at low stresses then an S-shape dependence appears. Thus it can be concluded, in contrast to the very frequently used approximation in the literature [9,20,21] about linear Calusius-Clapeyron relations, that the σ dependent ϵ^{tr} usually leads to nonlinear dependence [18,19]. Of course in special cases, i.e. when the dependence of ϵ^{tr} in the investigated range is weak, or the stress interval wide enough to have many points belonging to the saturation value of ϵ^{tr} a linear fit with an effective slope can be made, like in Figure 8. The slope of this straight line is 0.90 K/MPa,

which corresponds to an effective constant ε^{tr} value in equation (10) equal to 0.065 ($\Delta s = -7.2 \times 10^4 \text{ J/Km}^{-3}$ [18]), which is a bit larger than $\varepsilon^{tr}_{sat} = 0.061$ [18,19].

Closing this section Figure 9 shows the stress dependence of the transformation strain in polycrystalline Cu-20at%Al-2.2at%Ni-0.5%B alloy [6,22] for β/β' transformation. It can be seen that here ε_T is zero. Indeed, quite frequently in polycrystalline samples (see also [14,15]) ε_T is zero or close to zero and it can also happen that the saturation can not be reached in the σ interval investigated (as it is the case here as well).

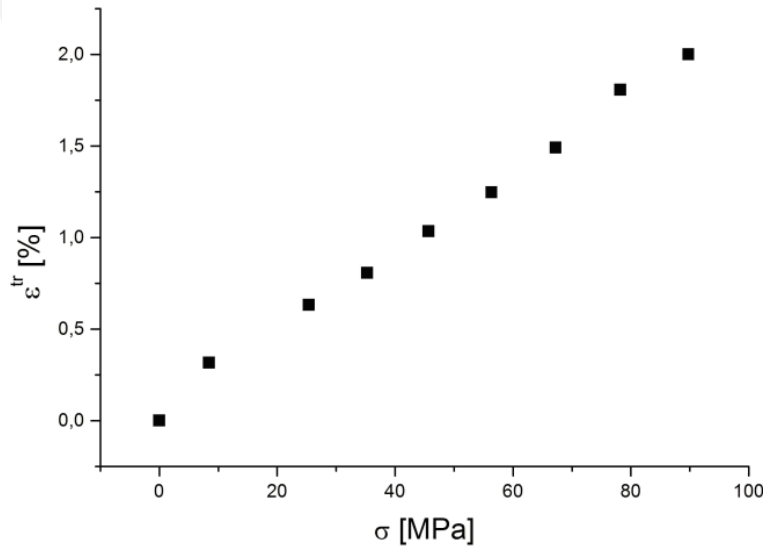


Figure 9. $\varepsilon^{tr}(\sigma)$ function for β/β' transformation in polycrystalline samples [6, 22].

3.3. Dependence of the derivatives of the elastic and dissipative energy contributions on the martensite volume fraction

As it was pointed out in Section 2 equations (13), (14) and (16), (17) offer the possibility to calculate the dependence of d and the $2T_0(\sigma) - 2e(\xi)/(-\Delta s)$ terms (or the e term directly if T_0 is known) on the transformed martensite volume fraction. In the case of CuAl(17.9w%)Ni(2.6w%) single crystalline alloy we could determine both the equilibrium transformation temperature and the entropy thus Figure 10 shows the $d(\xi)$ as well as the $e(\xi)$ function, respectively for 171.5 MPa (high stress limit). It can be seen that indeed the elastic energy contributions is zero up to about $\xi_c = 0.37$ and then significantly increases with increasing ξ (see also Figure 6) indicating that there is an elastic energy accumulation in this stage. Furthermore, since we have different shapes of the hysteresis loops at low and high stress limits (see also Figures 6), Figure 11 shows the $e(\xi)$ function at 42.4 MPa for the cooling down process. It is worth mentioning that a detailed analysis (see [5]) shows that the unusual shape of the loop at this stress level indicated (see Figure 12 which shows the inverse of the $T(\xi)$ loop obtained at 42.4 MPa: the sums and differences of the cooling and heating branches give the ξ dependence of the elastic and dissipative terms, respectively) that the elastic energy accumulation was practically zero up to about $\xi = 0.63$ during cooling and again zero for heating but, surprisingly now from $\xi = 1$ down to $\xi = 0.37$.

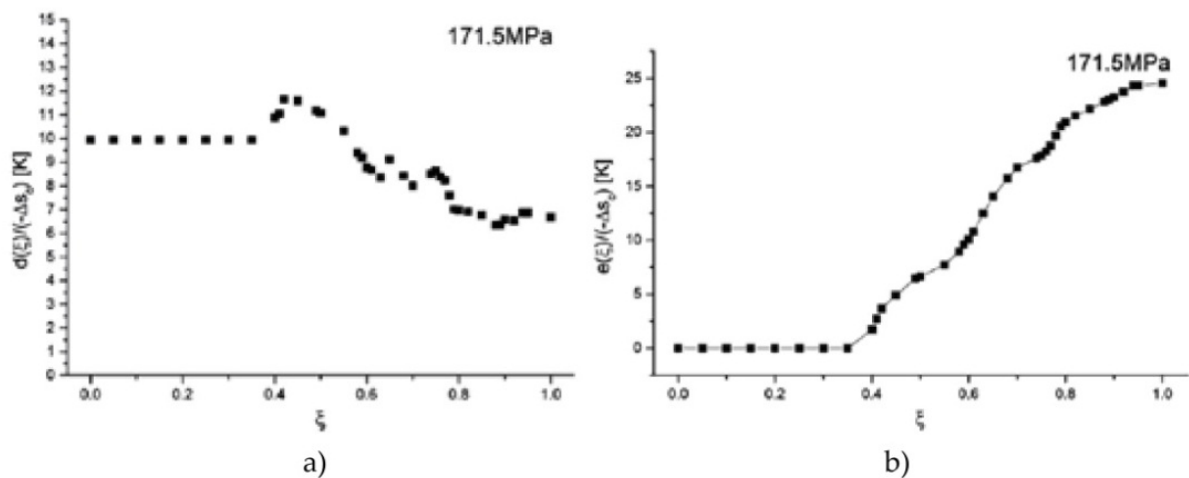


Figure 10. Derivative of the dissipative (left) and elastic energy (right) contributions versus transformed fraction in CuAl(17.9w%)Ni(2.6w%) single crystalline alloy for β/γ transformation at 171.5 MPa (high stress limit) [5].

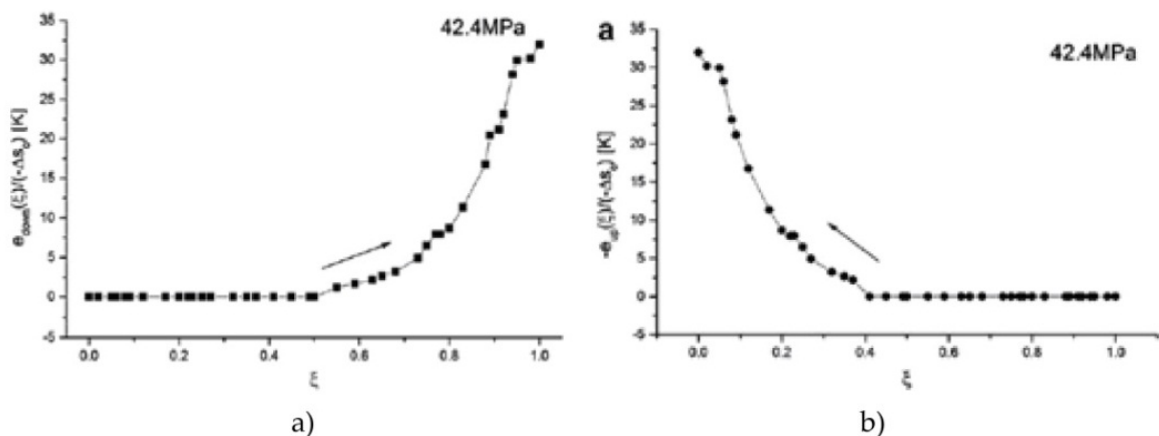


Figure 11. Derivative of the elastic energy versus the transformed fraction in CuAl(17.9w%)Ni(2.6w%) single crystalline alloy for β/γ transformation at 42.4 MPa (low stress limit) for cooling down (left) and heating up (right; in obtaining this curve a mirror transformation was made i.e. $-e^\uparrow(\xi=0)=e^\downarrow((\xi=1))$ and $-e^\uparrow(\xi=0.37)=e^\downarrow((\xi=0.63))$) [5].

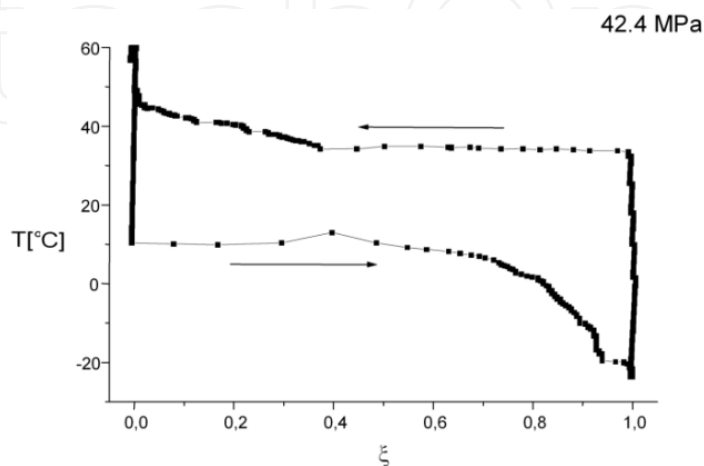


Figure 12. Inverse of the thermal loop shown on Fig. 6.

The above behaviour can be understood as follows [5]: under high stress levels the stress will prefer the nucleation of special variant(s), which can freely grow without the accumulation of elastic energy at the beginning and during cooling the relaxation of the stress starts from $\xi=1$ and after a certain value the elastic contribution will be zero. This is what was usually observed in martensitic transformations and can be described as “the first plate of martensite to form during cooling is usually the last plate of martensite to revert on heating” [1]. Thus in this case obviously after $\xi > \xi_c^\downarrow$ the elastic fields of the growing martensite variants will overlap (or in addition to the single growing variant, new nuclei can also form) and accumulation of the elastic energy takes place. On heating the reverse phenomenon (i.e. first the last martensite plates start to revert and the relaxation of the stored elastic energy between $\xi=1$ and $\xi=\xi_c^\downarrow$ takes place) can be observed. On the other hand curves at low stress levels showed different features. Indeed the multiple interface transformation takes place in the form as described above only in bulk samples and as stated in [1] “for other shapes of the same crystal (say, thin discs) the reverse transformation may nucleate competitively at separate places”. Indeed in [5] the samples had a form of rod with a relatively small cross-section. In this case there are no preferred martensite variants (if the stress level is too low and is in the order of magnitude of the internal random stress field) and the first martensite nuclei can appear at easy nucleation places (e.g. tips, edges). Nevertheless, at the beginning (around M_s) of cooling down, there is no change in the elastic energy (i.e. e is approximately zero) up to a certain value of ξ_c^\downarrow (either because the transformation takes place in a single interface mode, or because the elastic fields of the formed nuclei does not overlap yet). Obviously, for $\xi > \xi_c^\downarrow$ the elastic fields of the martensites formed start to overlap and accumulation of the elastic energy takes place. Thus this forward part of the transformation is very similar to that observed at high tensile stresses. In the reverse process the heating up branch of the hysteresis curve indicates that the first austenite particles may nucleate competitively at easy nucleation places (where the first martensite nuclei were formed during cooling) and thus at A_s the change in the elastic energy can be negligible. Indeed, as optical microscopic observations confirmed [5], the formation of surface relief at low stress level (at about $\sigma=0$) in the backward transformation usually started at places where the formation of the first martensite plates occurred (and not at places where their formation finished). Thus Figure 11 (on the right) shows the $e(\xi)$ for the heating up branch, but by using a mirror transformation (for the details see [5]).

Figure 13 shows the $d(\xi)=d^l(\xi)=d^h(\xi)$ as well as the $e(\xi)=e^l(\xi)=-e^h(\xi)$ functions in single crystalline samples for β/β' transformations [18], respectively. Since in this case we were not able to determine T_0 the elastic energy derivative contains also the constant term $2T_0(\sigma)\Delta s$ (see eq.(14)).

In Figure 14 the $d(\xi)=d^l(\xi)=d^h(\xi)$ as well as the $e(\xi)=e^l(\xi)=-e^h(\xi)$ functions are shown for polycrystalline Cu-20at%Al-2.2at%Ni-0.5%B alloy (β/β' transformation) [22]. Here again the elastic energy derivative contains the constant $2T_0(\sigma)\Delta s$ term.

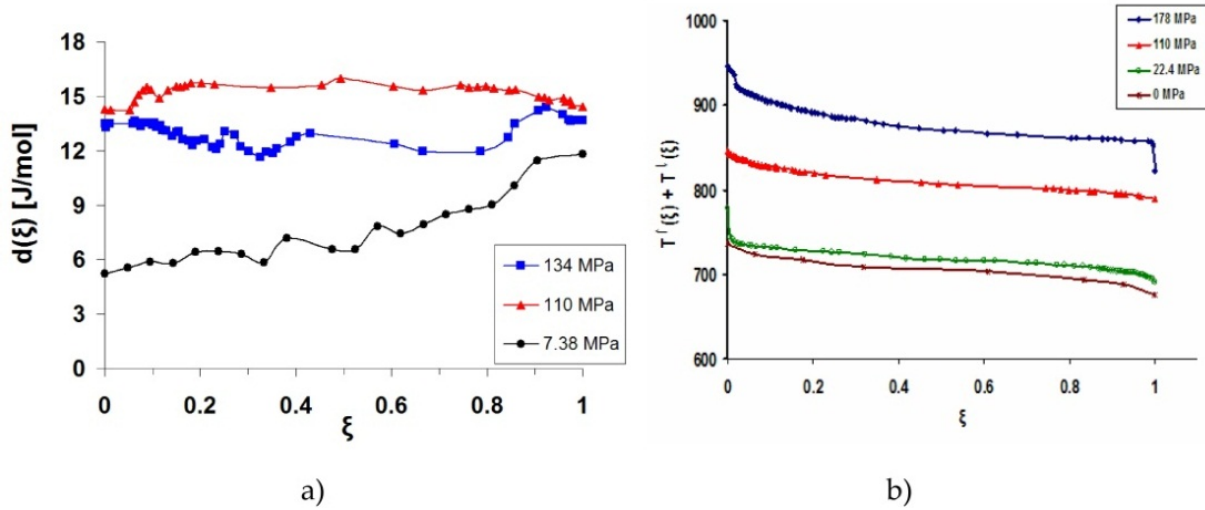


Figure 13. Dissipative (left) and elastic (right) energy terms versus the transformed martensite fraction for β/β' transformation in single crystalline samples [18], respectively. On the right only the difference of equations (6) are shown because $T_0(\sigma)$ is not known (see also the text).

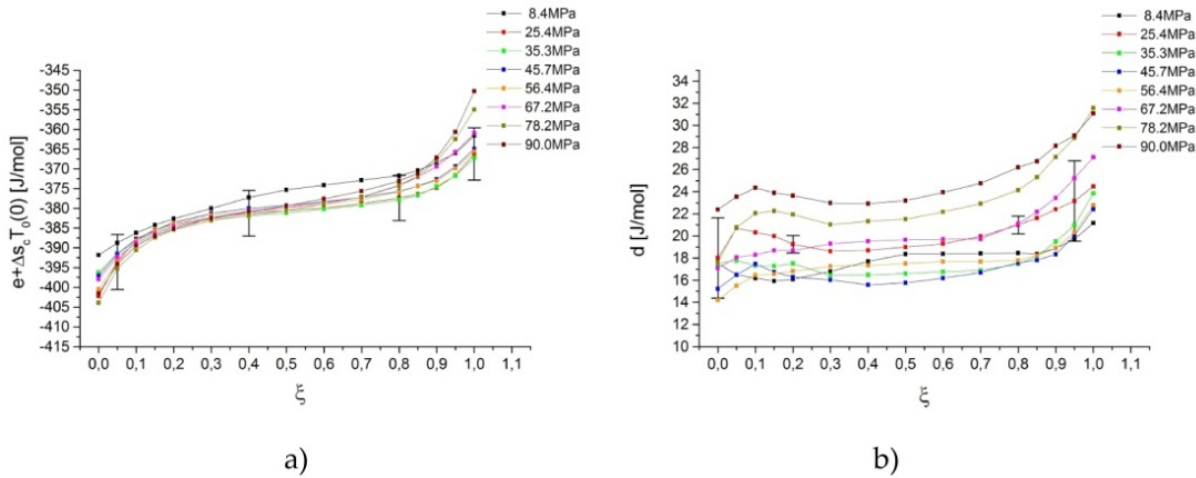


Figure 14. Elastic (left) and dissipative (right) energy terms versus ξ at different stress levels in polycrystalline $\text{Cu-20at\%Al-2.2at\%Ni-0.5\%B}$ alloy for β/β' transformation [22].

3.4. Stress and temperature dependence of the elastic and dissipative terms

We have seen that the relations presented in Section 2 allow calculating the stress as well as temperature dependence of the derivatives of the elastic or dissipative energies, at a fixed ξ value, or their integrals, i.e. the E and D quantities, from the $\xi \sim T$, as well as from the $\xi \sim \sigma$ loops, respectively. Let us see these functions for the three alloys investigated.

In the single crystalline $\text{CuAl(17.9w\%)Ni(2.6w\%)}$ samples (β/γ transformation) the dissipative energy contributions were calculated from the parallel parts of the loops (see Figure 6), using that d is independent of ξ here. These values can be seen in Figure 15 as the function of the applied stress [5, 22]. It shows a slight maximum at around 90 MPa, i.e. there are increasing and decreasing tendencies in the low and the high stress range, respectively.

Figure 16 shows the full dissipated energy and stored elastic energy in martensitic state as the function of applied stress. It can be seen that the dissipative energy slightly decreases while the elastic one increases with increasing stress. This is similar to the behaviour observed in NiTi single crystals in [23].

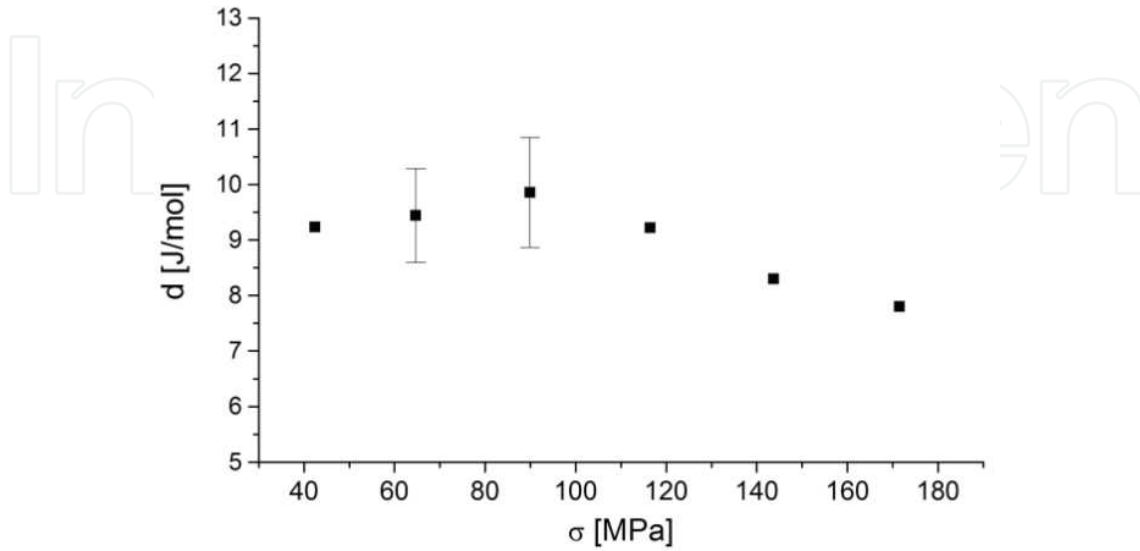


Figure 15. Stress dependence of the derivative of the dissipative energy calculated from the ξ intervals of the thermals loops where the two branches were parallel to each other [5,22] in single crystalline CuAl(17.9w%)Ni(2.6w%) samples (β/γ transformation).

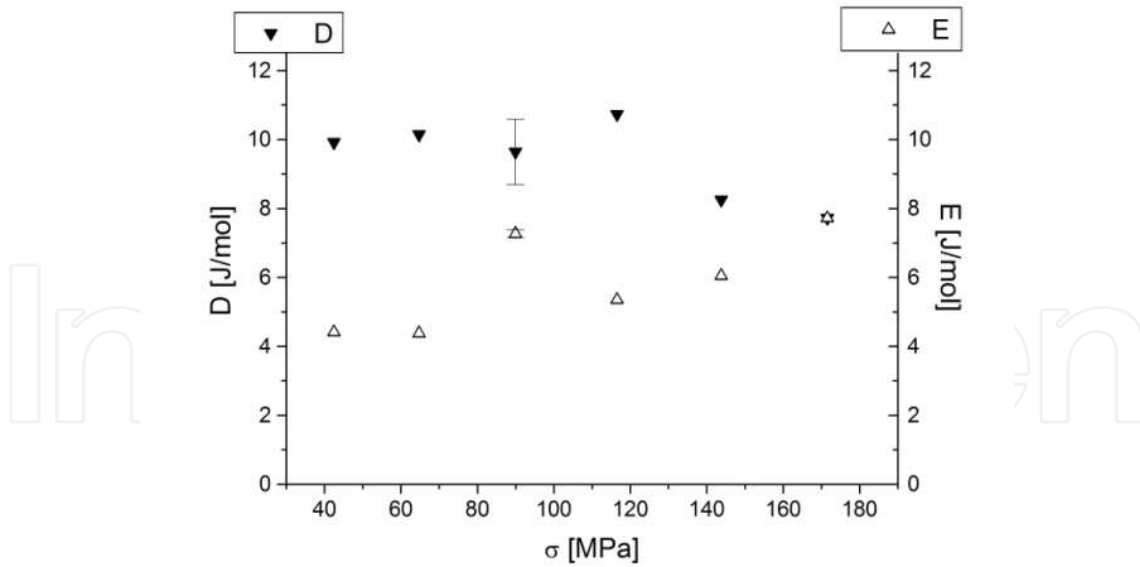


Figure 16. Stress dependence of the integral values of the dissipative and elastic energies [5,22] in single crystalline CuAl(17.9w%)Ni(2.6w%) samples (β/γ transformation).

In single crystalline CuAl(11.5wt%)Ni(5.0wt%) alloys (β/β' transformation) the stress dependence of e and d quantities at fixed values of ξ (at $\xi=1$ and $\xi=0$, denoted by indexes 1 and 0, respectively) is shown in Figure 17, while Figure 18 illustrates the temperature

dependence of them. Furthermore in Figure 19 and 20 the total dissipative and elastic energies are shown as the function of σ as well as T . It can be seen from Figure 17 that, although the scatter of points is rather high, the d_i ($i=1, 0$) terms can have a maximum at around 60 MPa, while their average value at the low and high stress values is 7 J/mol [18]. On the other hand the elastic energy term has definite stress dependence with the slopes -0.25 and -0.14 J/molMPa for e_0 and e_1 , respectively. Furthermore, both the elastic and dissipative terms have linear temperature dependence (Figure 18) with the following slopes: $\partial e_0/\partial T=-0.50$ J/molK, $\partial e_1/\partial T=-0.18$ J/molK, and $\partial d_0/\partial T \cong \partial d_1/\partial T=-0.028$ J/molK [18, 24]. Thus it is not surprising that in Figure 19 the dissipative energy D has a maximum at about 60 MPa and the elastic energy, E , has linear stress dependence (decreases with increasing stress), while in Figure 20 the D versus T function is almost constant and E has a negative slope too.

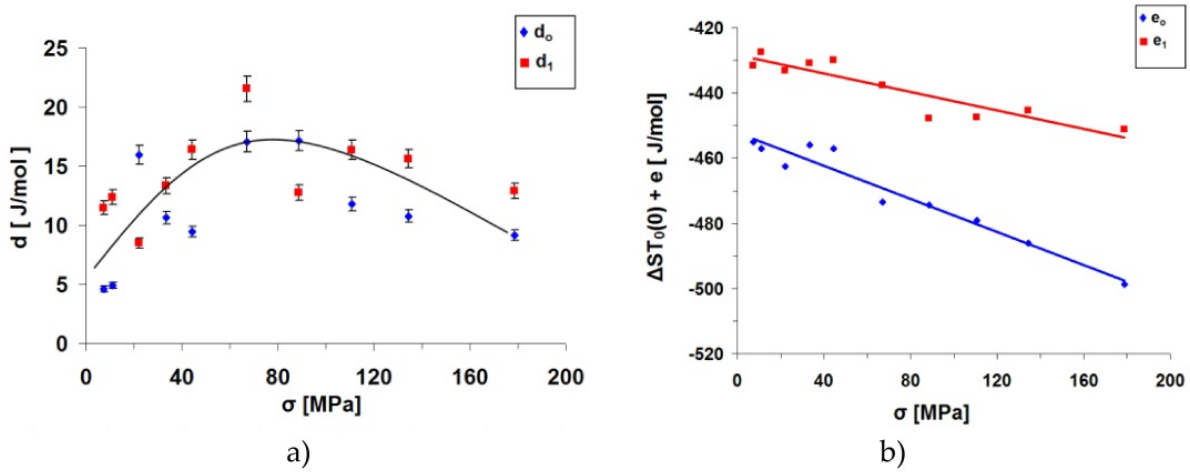


Figure 17. Stress dependence of the of the derivatives of the dissipative (left) and elastic (right) energies at $\xi=1$ and $\xi=0$ in single crystalline CuAl(11.5wt%)Ni(5.0wt%) alloys (β/β' transformation) [18].

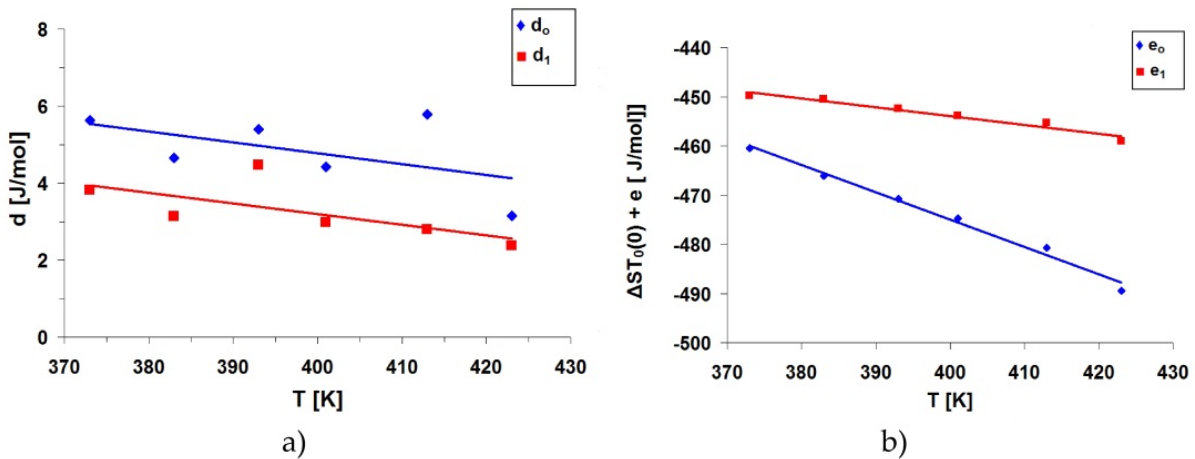


Figure 18. Temperature dependence of the of the derivatives of the dissipative (left) and elastic (right) energies at $\xi=1$ and $\xi=0$ in single crystalline CuAl(11.5wt%)Ni(5.0wt%) alloys (β/β' transformation) [18, 24].

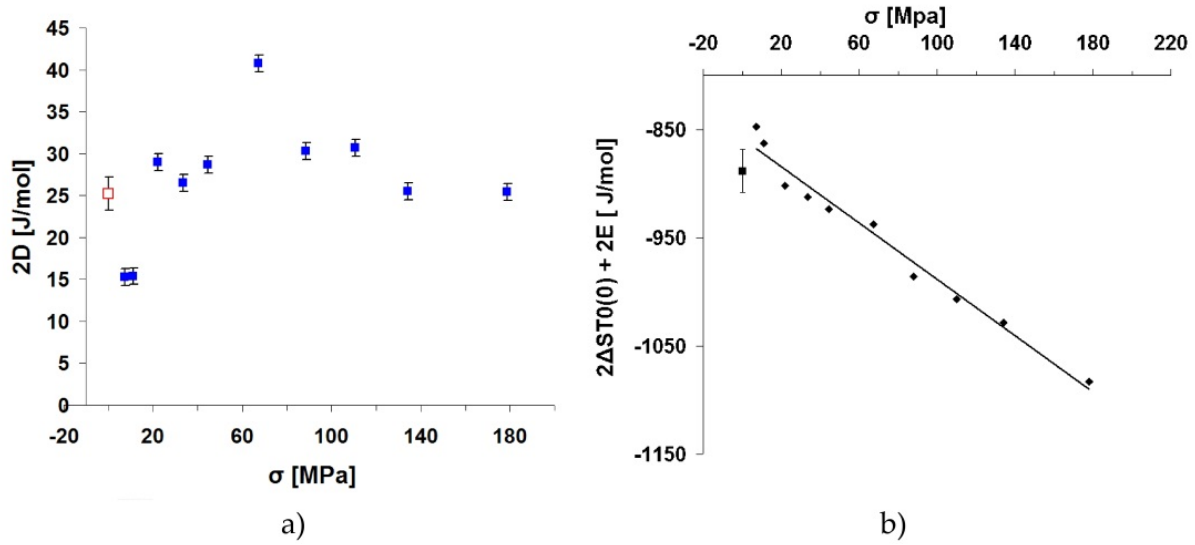


Figure 19. Total dissipative (left) and elastic (right) energies as the function of stress in single crystalline CuAl(11.5wt%)Ni(5.0wt%) alloys (β/β' transformation) [18].

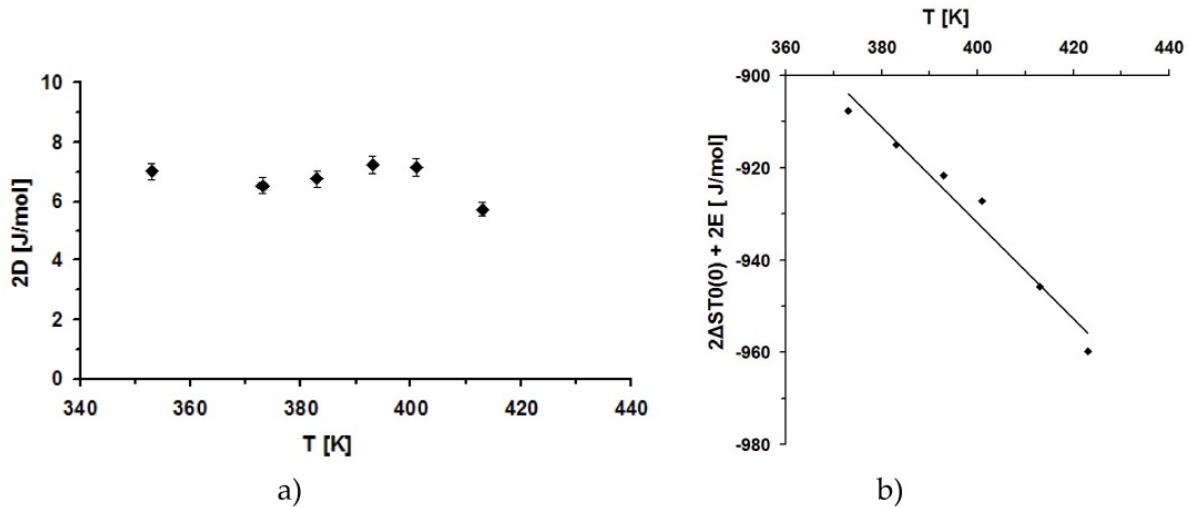


Figure 20. Total dissipative (left) and elastic (right) energies as the function of temperature in single crystalline CuAl(11.5wt%)Ni(5.0wt%) alloys (β/β' transformation) [18].

The values obtained for the d_o and d_1 (and D) quantities are almost the same values in both sets, but their value is lower for the $\sigma \sim \varepsilon$ loops by a factor of 3. Nevertheless, the average value on the d_i versus σ plots at low and high stresses (~ 7 J/mol) is close to 4 J/mol obtained from the $d_i(T)$ functions. Furthermore, since at higher temperatures higher stress is necessary to start the transformation, it is also plausible that the negative slope of the second part on Figure 17 should correspond to a negative slope on the $d_i(T)$ functions. Indeed there is a slight decreasing tendency with increasing T on Figure 18. Unfortunately, the accuracy of our present results does not allow a deeper and proper analysis of the field dependence of the dissipative terms. In addition, the details of the transformation (and thus the magnitude of d_i) can be different for stress and temperature induced transformations as well as can also depend on the prehistory of the samples (not investigated here).

In polycrystalline Cu-20at%Al-2.2at%Ni-0.5%B samples (β/β' transformation) [3,22] Figures 21 and 22 show the stress dependence of the d_i , e_i as well as D and E quantities, respectively.

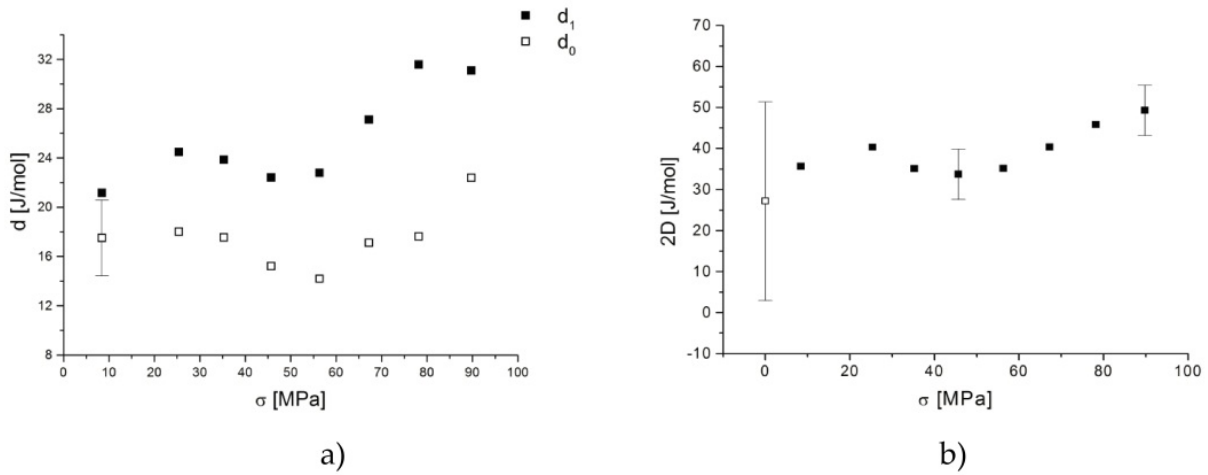


Figure 21. Stress dependence of the derivatives of the dissipative (left) and elastic (right) energies at $\xi=1$ and $\xi=0$ in polycrystalline Cu-20at%Al-2.2at%Ni-0.5%B samples (β/β' transformation) [3, 22].

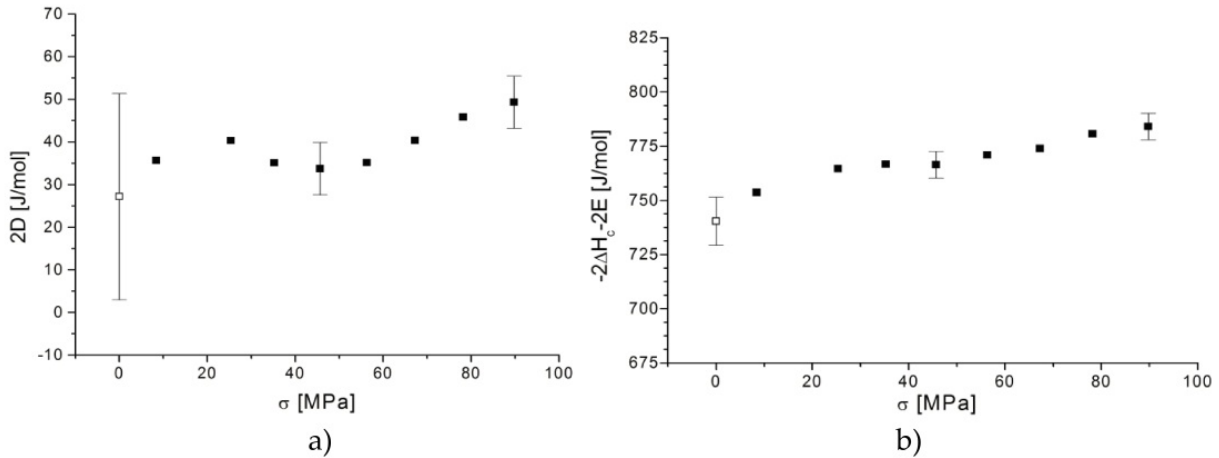


Figure 22. Stress dependence of the dissipative (left) and elastic (right) energies at $\xi=1$ and $\xi=0$ in polycrystalline Cu-20at%Al-2.2at%Ni-0.5%B samples (β/β' transformation) [3, 22].

Closing this subsection it is worth mentioning two more aspects. One is the self-consistency of our analysis. The dots at $\sigma=0$ in Figures 19 and 22 show the values calculated from the DSC curves, according to the relations (24) and (25). Thus e.g. $Q^\downarrow + Q^\uparrow = 2D = 25$ J/mol ($Q^\downarrow = -331.6$ J/mol, $Q^\uparrow = 357.6$ J/mol [18]) in Figure 19. It can be seen that these dots fit self-consistently within the experimental errors to the other dots calculated from the independent (hysteresis loops) measurement. The another point is related to the connection between the stress and temperature dependence of ε^tr (i.e. the change of the martensite variant structure) and the stress and temperature dependence of the characteristic parameters of the hysteresis loops in single crystalline samples. Although

this point will be analyzed in detail in the next subsection too, it is worth summarizing some qualitative correlations: i) as it can be seen from Figure 5 as well as Figures 15 and 16 the E and D quantities change in the same stress interval where ε^{tr} for the β/γ transformation, ii) a very similar relation can be observed between ε^{tr} (Figure 3b) and d as well as D for β/β' transformation (Figures 17 and 19).

3.5. Stress and temperature dependence of the start and finish temperatures and stresses, respectively

3.5.1. Stress dependence of the start and finish temperatures

It is worth investigating whether the commonly used assumption in the literature (see e.g. [9, 25, 26]) that the slopes of the start and finish temperatures and the slope of the $T_0(\sigma)$ are approximately the same or not. From the relations, presented in Section 2, it is clear that i) strictly even the linear σ dependence of T_0 is not fulfilled in general (see e.g. Figure 3b which illustrates that ε^{tr} is not constant), ii) the σ dependence of the elastic and dissipative terms (e_i , d_i , $i = 0,1$) as compared to the $T_0(\sigma)$ function, can also give a contribution to the stress dependence of the start and finish temperatures (see relations (18)). Such an analysis was carried out for the results obtained in single crystalline CuAl(11.5wt%)Ni(5.0wt%) alloys (β/β' transformation) in [18] and will be summarized here. As we have already seen in Figure 8 the $T_0(\sigma)-T_0(0)$ function can be approximated by a straight line, neglecting the small deviations in the interval between 0 and 50 MPa. In fact this slight S-shape part up to 50 MPa is the consequence of the stress dependence of ε^{tr} (see the insert in Figure 8). The straight, line fitted in the whole stress range, gives the slope 0.39 ± 0.05 K/MPa. At the same time the slopes of M_s and A_f as well as M_f , and A_s (as shown in Figure 23, on the left) are almost the same: 0.59 as well as 0.50 K/MPa, respectively. Thus these differ from the one obtained for the slope of $T_0(\sigma)$. It should be decided whether this difference comes from the stress dependence of d_i or e_i parameters or from both. As it can be seen in Figure 17, although the d_i function indicates a maximum at around 60 MPa, from the point of view of the slope of this function in the whole stress interval, one can assume that within the scatter of the measured points they are independent of the stress. On the other hand the e_0 and e_1 parameters have a linear stress dependence with the slopes (see also above) - 0.25 and -0.14 J/molMPa for e_0 and e_1 , respectively. Dividing these by the value of Δs ($= -1.26$ J/Kmol [18]) the elastic energy contribution to the slope of the start and finish temperatures (see relations (18)) will be - 0.20 and - 0.11 K/MPa, respectively. Thus the differences in the slopes of the start and finish temperatures and the equilibrium transformation temperature are caused by the stress dependence of the derivative of the elastic energy contribution.

Finally it is worth mentioning that since both the stress dependence of $T_0(\sigma)$ and the elastic terms can be relatively well fitted by straight lines, it is not surprising that in the literature frequently a linear relation is found for the stress dependence of the start and finish temperatures.

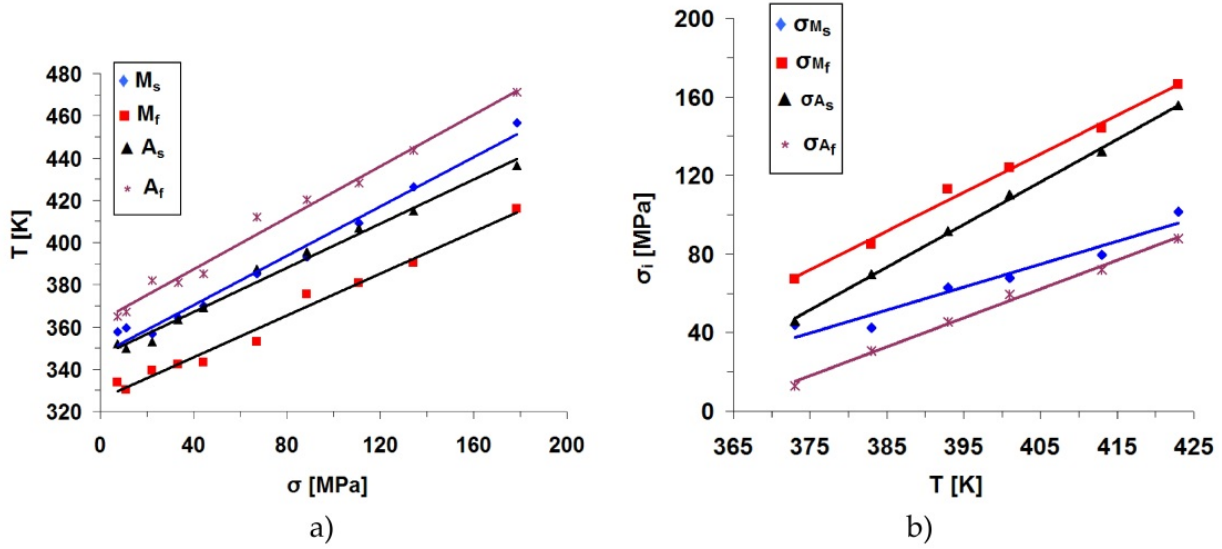


Figure 23. Stress dependence of the start and finish temperatures (left) and temperature dependence of the start and finish stresses (right) in single crystalline CuAl(11.5wt%)Ni(5.0wt%) alloys (β/β' transformation) [18].

3.5.2. Temperature dependence of the start and finish stresses [24]

In many papers about the relations between the start/finish stresses and the test temperature, T , in martensitic transformations of shape memory alloys it is assumed that e.g. the temperature dependence is the same as that of the $\sigma_o(T)$ function (σ_o is the equilibrium transformation stain). As we have seen the linearity of this (or the $T_o(\sigma)$ relation) Clausius-Clapeyron-type relation would be fulfilled only if the transformation strain, ε^tr , would be constant. Furthermore, it was illustrated in the previous section that relations between the start and finish temperatures versus stresses can contain stress dependent elastic and dissipative energy contributions. Thus even if these relations are approximately linear their slopes can be different from each other and from the slope of the $T_o(\sigma)$ function. The situation is very similar when one considers the $\sigma_o(T)$ as well as temperature dependence of the start and finish stresses.

In practice σ_{M_s} and σ_{A_s} are the most important parameters in thermomechanical treatments. Let us consider isothermal uniaxial loading tests carried out at temperatures $T > A_f$. In this case σ_{M_s} means the critical stress for the formation of stress induced martensite variants. In order to get expression for $\sigma_{M_s}(T)$ let us take the first relations of (18) (at $\sigma=0$) and (19) and make the use of (11) [24]:

$$\begin{aligned} \sigma_{M_s}(T) = & -(\Delta s / V \varepsilon^{tr}(\sigma_o(T))) [T - M_s(0)] + [1 / V \varepsilon^{tr}(\sigma_{M_s})] [d_o(\sigma_{M_s}) + e_o(\sigma_{M_s})] - \\ & - [d_o(0) + e_o(0)] [1 / V \varepsilon^{tr}(\sigma_o(T))]. \end{aligned} \quad (28)$$

Note that in the relations used in obtaining (28) the transformation strain and the transformed fraction derivatives of the dissipative and elastic terms were considered stress

dependent. It can be seen that relation (28) will have the form usually found in the literature (see e.g. [10,27]) only if the sum of the last two second terms is zero and, even in this case, it will have a linear temperature dependence only if $\varepsilon^{tr}(\sigma_o(T))$ is constant. Similar relations can be obtained for the other start and finish stresses. In the case of σ_{Mf} the sum of d_1 and e_1 appears and in the second term they should be taken at σ_{Mf} , while for σ_{Af} and σ_{As} the e_o-d_o as well as e_1-d_1 differences will be present. For example;

$$\sigma_{As}(T) = -(\Delta s / V \varepsilon^{tr}(\sigma_o(T))) [T - A_s(0)] + [1 / V \varepsilon^{tr}(\sigma_{As})] [e_1(\sigma_{As}) - d_1(\sigma_{As})] - [e_1(0) - d_1(0)] [1 / V \varepsilon^{tr}(\sigma_o(T))]. \quad (29)$$

One can recognize from (28) or (29) that interestingly if the contributions from the elastic and dissipative contributions are neglected the slopes of all start and finish stresses versus temperature have the same value (or have the same curvature).

Now the analysis of the experimental data obtained in single crystalline CuAl(11.5wt%)Ni(5.0wt%) alloys (β/β' transformation) resulted in the following results [24]. First it is interesting to recognize a correlation between the stress and temperature dependence of ε^{tr} : it can be seen from Figure 4a that e.g. at 373 K the martensite start stress is about 30 MPa and on the curve shown in Figure 3b this leads to about 4% ε^{tr} value, which is approximately the same as was observed at this temperature ((see Figure 4b). *Thus the transformation strain has indirect temperature dependence and it is the result of its σ -dependence.* It is easy to understand the above indirect temperature dependence: since in expression (2) the elastic and thermal terms play equivalent roles with opposite signs in the thermoelastic balance [8,9] at higher temperatures higher stress is necessary to start the transformation and the martensite structure formed will be more oriented at this higher temperature: η and thus ε^{tr} will be larger.

Next, let us see whether the slopes of the start and finish stresses versus temperature are the same or not. It can be seen in Figure 23 (on the right) that the functions can be approximated by straight lines and Table 1 contains their slopes. However, while the slopes of $\sigma_{Ms}(T)$ and $\sigma_{Af}(T)$ as well as $\sigma_{Mf}(T)$ and $\sigma_{As}(T)$ are the same the slopes of these two groups differ from each other more than the estimated error (about 0.05 MPa/K [18]).

In (28) and (29) both d_o and d_1 terms has a very moderate temperature dependence with the same slopes of (Figure 18) -0.028J/molK (leading to a small contribution to the slope of the temperature dependence of the start/finish temperatures as -0.064MPa/K) while $e_o(\sigma_{Ms}(T))$ depends on temperature (see Figure 23: $\partial e_o/\partial T = -0.50$ J/molK, $\partial e_1/\partial T = -0.18$ J/molK [18, 24]). Furthermore the $\varepsilon^{tr}(\sigma_o(T))$ and $\varepsilon^{tr}(\sigma_{Ms}(T))$ functions should be considered in the temperature interval 373-425K (Figures 23 and 4b) i.e., as an average value, one can take $\varepsilon^{tr}(\sigma_o(T)) \cong \varepsilon^{tr}(\sigma_{Ms}(T)) \cong 0.055$. Thus the terms containing $1/V\varepsilon^{tr}$ will be approximately constant $1/V\varepsilon^{tr} \cong 2.3 \times 10^6$ mol/m³ (a bit larger than the value belonging to ε^{tr}_{max} : 2.1×10^6 mol/m³, $V = 7.9 \times 10^{-6}$ m³/mol [18]).

Thus, one can estimate the contributions of the 1st, 2nd and 3rd terms in (28) and (29) to the slope of σ_{Ms} and σ_{As} vs. T functions (Table 1). The slope of the third term is 0 ($\varepsilon^{tr}(\sigma_o(T)) \cong \varepsilon^{tr}(\sigma_{Ms}(T)) \cong \text{const.}$) and from the second term the elastic term gives determining

contribution to the slope. This also explains why the slopes of σ_{Ms} and σ_{Af} as well as σ_{Mf} and σ_{As} are similar, because they contain the different temperature derivatives of e_0 and e_1 , respectively.

Experimental vales [18]	σ_{Ms} vs. T	σ_{Mf} vs. T	σ_{Af} vs. T	σ_{As} vs. T
Slope in MPa/K	1.6	2.0	1.5	2.2

Estimated (parts)	Eq. (11)	1st term in (28) and (29)	2nd term in (28), e_0	2nd term in (29) e_1	3rd term in (28) or (29) $d_0=d_i$
Slope in MPa/K	2.59	2.83	-1.15	-0.41	-0.06

Estimated (whole)	σ_{Ms} vs. T	σ_{Mf} vs. T	σ_{Af} vs. T	σ_{As} vs. T
Slope in MPa/K	1,6	2.3	1.7	2.5

Table 1. Experimental and estimated values of the slopes of the start and finish stresses versus T [24].

It can be seen from Table 1 that taking all the contributions into account the agreement between the estimated and experimental values is very good.

Finally a comment, similar to that given at the end of Section 2.5.1., can be made here too: since both the $\sigma(T)$ and the temperature dependence of the elastic terms (giving the determining contribution to the T dependence) can be well approximated by straight lines, the linear relations between the start and finish stresses and the test temperature can be frequently linear.

3.6. Effect of cycling

After the illustration of the usefulness of the above model in the calculation of the elastic and dissipative energy contributions from hysteresis loops of thermal and mechanical cycling in this section the results on the effect of number of the above cycles on the energy contributions will be summarized.

In [17] the effect of thermal and mechanical cycling on β/β' phase transformation in CuAl(11.5W%)Ni(5.0W%) single crystalline shape memory alloy was studied. The $\sigma\sim\varepsilon$ and $\xi\sim T$ hysteresis loops were investigated after different numbers of thermal and mechanical cycles. The $\sigma\sim\varepsilon$ loops were determined at fixed temperature (373 K) and the $\xi\sim T$ loop under zero stress was calculated from the DSC curves measured.

Figure 24 (left) shows the ξ - T loops, calculated from the DSC curves, after different numbers of cycles, N , and the N dependence of the start and finish temperatures (right). Figure 25 illustrates the N dependence of the start and finish stresses, while in Figures 26 and 27 the N dependence of the calculated dissipative and elastic energies are shown as calculated from the thermal and mechanical cycling.

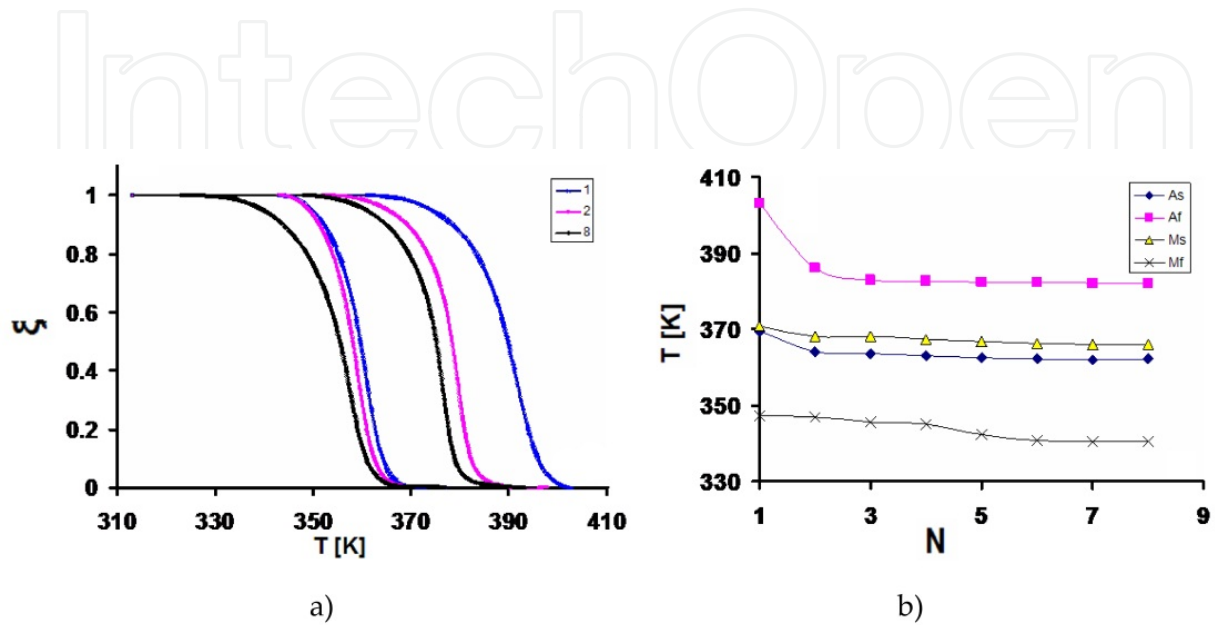


Figure 24. ξ - T loops (left), calculated from the DSC curves, after different numbers of cycles, N , in CuAl(11.5W%)Ni(5.0W%) single crystalline alloy and the N dependence of the start and finish temperatures (right) [17].

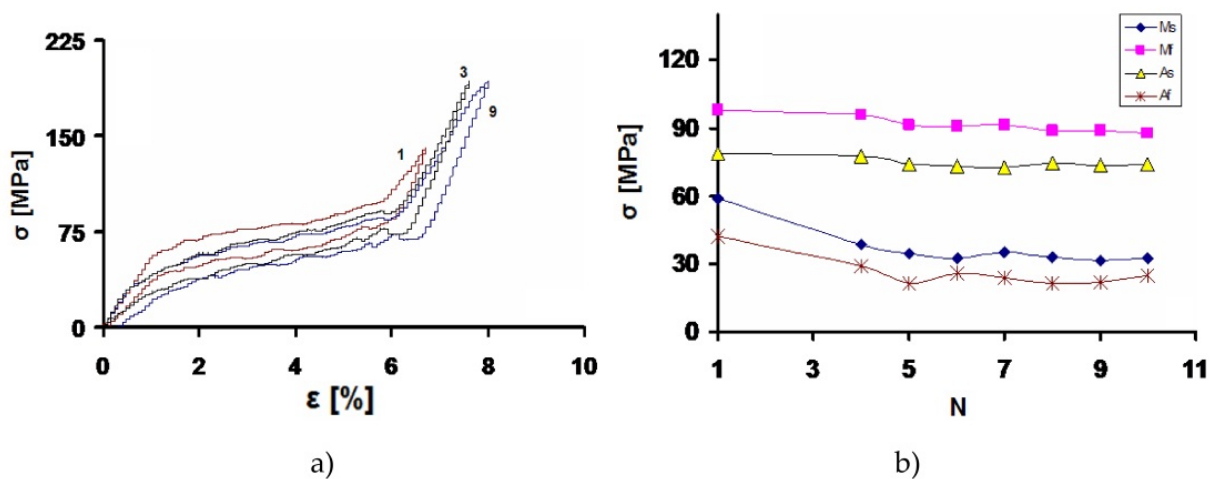


Figure 25. σ ~ ϵ loops (left) after different numbers of cycles, N , and the N dependence of the start and finish stresses in CuAl(11.5W%)Ni(5.0W%) single crystalline alloy (right) [17].

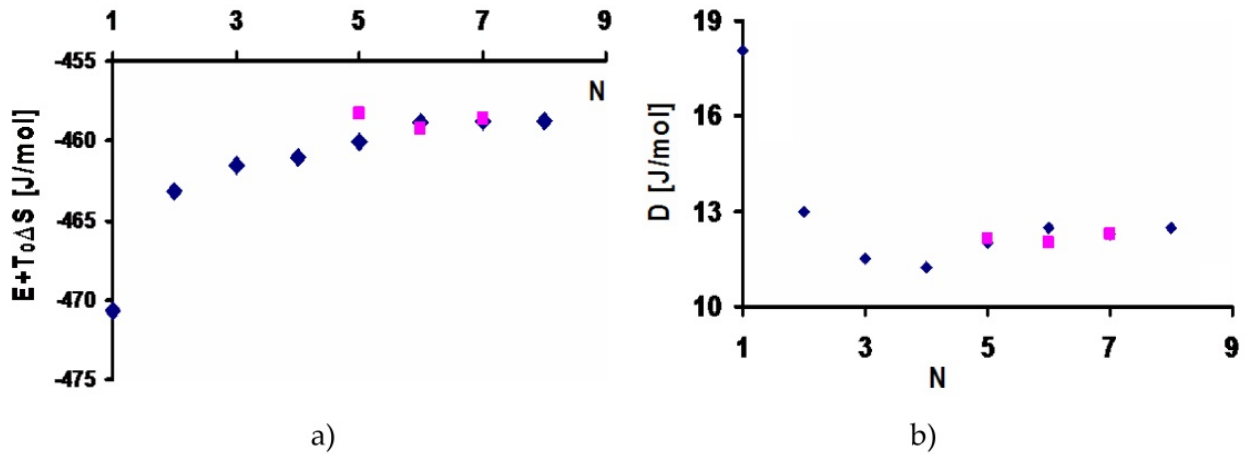


Figure 26. Cycle number dependence of the total elastic energy (left) and the total dissipative energy (right) for thermal cycles (♦ obtained from the ξ - T loops, ■ obtained from the heats of transformation) in CuAl(11.5W%)Ni(5.0W%) single crystalline alloy (right) [17].

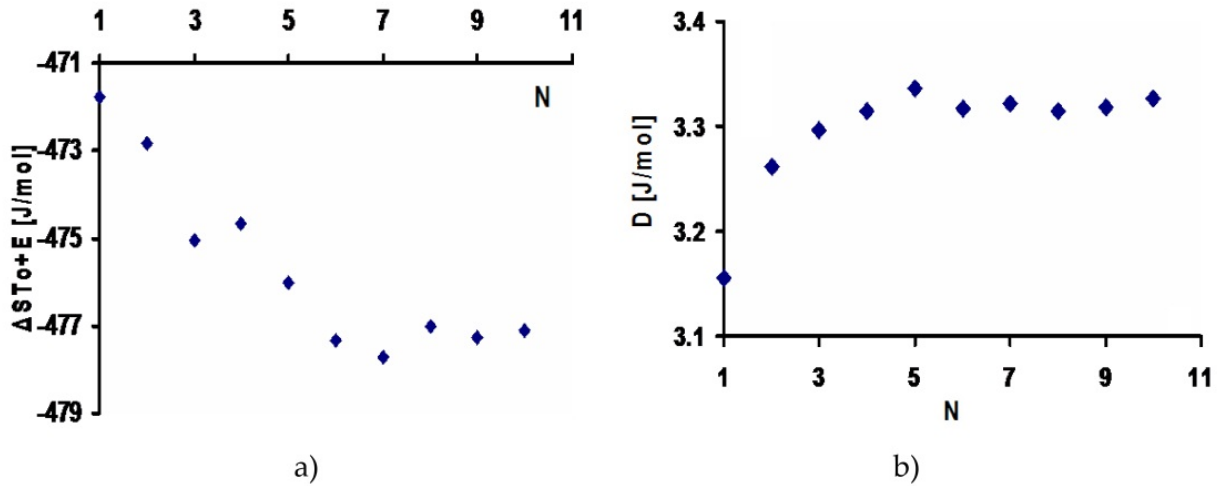


Figure 27. Cycle number dependence of the total elastic energy (left) and the total dissipative energy (right) for mechanical cycles in CuAl(11.5W%)Ni(5.0W%) single crystalline alloy (right) [17].

From the results presented in Figures 24-27 the following conclusions can be drawn [17]:

- Both the thermal and mechanical cycling causes some changes in the hysteresis loops: after a fast shift in the first few cycles the stress-strain and strain-temperature response stabilize.
- In thermal cycling the elastic energy, E , as well as the dissipative energy, D (per one cycle), increases as well as decreases, respectively with increasing number of cycles, while in mechanical cycling there is an opposite tendency. These changes are inevitably related to the change in the martensite variant structure during cycling.
- In thermal cycling, where self-accommodated martensite variant structure develops, with increasing numbers of N , due to some "learning process in nucleation of similar variants" at different places, the martensite variant structure stabilizes and interestingly in this process E increases (by about 2.5%) and D decreases (by about 50 %).

- iv. In mechanical cycling it is expected that the learning process can lead to an increased number of nucleation of preferentially oriented (according to the direction of the applied uniaxial stress) martensite variants. This decreased E and increased D by about 1 % and 6% respectively.
- v. In general there are two energy dissipative processes [23]: the first is related to the frictional interfacial motion, while the second is due to the dissipation of the stored elastic energy when the coherency strains at the martensite/austenite interface relax. Assuming the first contribution independent of N , the increase/decrease of E can be accompanied by a decrease/increase in D , but for a deeper understanding detailed microscopic investigation of the variant structure and the interfaces, similarly as e.g. was done in [23], is necessary.

4. Conclusions

The analysis of extended experimental data obtained in poly- and single crystalline Cu based alloys provided the following main conclusions:

1. It has been illustrated that the transformation strain, ε^T , depends on both the uniaxial stress and temperature in measurements carried out in single crystalline samples at different constant stress and temperature values, respectively. In both functions the saturation values were the same corresponding to the maximal possible transformation strain, ε_{max}^T , estimated for the case when a single crystal fully transforms to the most preferably oriented martensite. This behaviour was interpreted by the change of the martensite variant structure as the function of the parameter, η , the volume fraction of the stress induced (single) variant martensite structure. In the $\varepsilon^T = \varepsilon_T + (\varepsilon_\sigma - \varepsilon_T)\eta$ relation ε_T and ε_σ are the transformation strains when fully thermally induced multi variant structure forms ($\eta=0$), as well as when the martensite consists of a fully ordered array of stress preferred variants (single variant state, $\eta=1$), respectively. It has been illustrated that ε_T can be either zero or can have a finite value (remanent strain) depending on the details of the variant structure (and thus on the prehistory of the sample).
2. The stress and temperature dependence of ε^T (or η) is reflected in deviations from the Clausius-Clapeyron-type relations. Indeed it was demonstrated that the equilibrium transformation temperature, T_0 , was not a linear function of the stress in single crystalline alloys.
3. Using relations for the $\xi \sim T$ and $\sigma \sim \varepsilon$ ($\varepsilon \sim \xi$) loops (ξ is the transformed martensite volume fraction) the ξ dependence of the ξ derivatives of the elastic and dissipative energies, $e(\xi)$ and $d(\xi)$ could be determined. The integrals of these functions gave the elastic, E , and dissipative, D , energies per on cycle. Thus it was also possible to determine their dependence on the stress and temperature. Note that the σ or T dependence of the elastic energy can be calculated only exclusive of a constant term containing the product of the entropy and $T(\sigma=0)$ (see eqs. (10), (13) and (16)). In the CuAl(17.9w%)Ni(2.6w%) single crystalline alloy, by the analysis of the peculiar shapes of the $\xi \sim T$ loops even the determination of the equilibrium transformation temperature and its σ dependence was possible. It was also demonstrated that our procedure is self-

consistent since e.g. at zero stress the D and E quantities were also calculated from independent measurements (DSC curves) and the results were in very good agreement with those values obtained from the integrals of the $e(\xi)$ and $d(\xi)$ functions.

4. It was shown that the stress and temperature dependence of ε^T (or η) is also reflected in the shape of the $D(\sigma)$, $D(T)$, $E(\sigma)$ and $E(T)$ functions, since these terms should be plausibly dependent on the martensite variant structure developed.
5. It was illustrated that both the stress dependence of the start and finish temperatures as well as the temperature dependence of the start and finish stresses in general can be approximated by straight lines. This is due to the facts that the $T_o(\sigma)$, $\sigma_o(T)$ functions, in a wider interval of their variables, can be linear as well as the elastic energy contributions (giving dominating contributions to the σ or T dependence) can also be fitted by a linear functions. On the other hand, the slopes of the start and finish parameters as well as the slopes of the $T_o(\sigma)$ or $\sigma_o(T)$ can be definitely different from each other.

It was shown that the number of thermal and mechanical cycling, N , has effected the values of E and D : in thermal cycling E increased, while D decreased with N . During mechanical cycling an opposite effect was observed.

Author details

Dezso L. Beke, Lajos Daróczy and Tarek Y. Elrasasi

Department of Solid State Physics, University of Debrecen, Debrecen, Hungary

Acknowledgement

This work has been supported by the Hungarian Scientific Research Found (OTKA) project No. K 84065 as well as by the TÁMOP-4.2.2/B-10/1-2010-0024 project which is co-financed by the European Union and the European Social Fund.

5. References

- [1] Salzbrenner R J, Cohen M (1979) On the thermodynamics of thermoelastic martensitic transformations. *Acta Metall.* 27: 739-748.
- [2] Tong H C, Wayman C M (1974) Characteristic temperatures and other properties of thermoelastic martensites. *Acta Metall.* 22: 887-896.
- [3] Palánki Z, Daróczy L, Beke D L (2005) Method for the determination of non-chemical free energy contributions as a function of the transformed fraction at different stress levels in shape memory alloys. *Mater. Trans.* A46: 978-982.
- [4] Daróczy L, Beke D L, Lexcelent C, Mertinger V (2004) Effect of hydrostatic pressure on the martensitic transformation in CuZnAl(Mn) shape memory alloys. *Scripta Mat.* 43:691- 697.
- [5] Palánki Z, Daróczy L, Lexcelent L, Beke D L (2007) Determination of the equilibrium transformation temperature (T_o) and analysis of the non-chemical energy terms in a CuAlNi single crystalline shape memory alloy. *Acta Mat.* 55: 1823-1830.

- [6] Daróczy L, Palánki Z, Szabó S, Beke D L (2004) Stress dependence of non-chemical free energy contributions in Cu–Al–Ni shape memory alloy. *Material Sci. and Eng.* A378: 274-277.
- [7] Beke D L, Daróczy L, Lexcelent C, Mertinger V (2004) Determination of stress dependence of elastic and dissipative energy terms of martensitic phase transformations in a NiTi shape memory alloy. *Journal de Physique IV (France)* 115: 279-285.
- [8] Beke D L, Daróczy L, Palánki Z (2008) On relations between the transformation temperatures, stresses, pressures and magnetic fields in shape memory alloys. in S. Miyazaki editor. *Proc. of Int. Conf. on Shape Memory and Superelastic Technologies*, 2007, Tsukuba, Japan, (ASM International, Materials Park, Ohio) pp. 607-614.
- [9] Planes A, Castan T, Ortin J, Delaey L (1989) State equation for shape memory alloys: Application to Cu Zn Al. *J. Appl. Phys.* 66(6): 2342-1348
- [10] Delaey L (1991) Diffusionless transformations. in Cahn R W, Haasen P, Kramer E J, editors. *Materials Science and Technology – A Comprehensive Treatment Vol. 5., Chp.5* in Haasen P, editor. *Phase Transformations in Materials*: Weinheim, VCH, p. 339
- [11] Tanaka K, Sato Y (1986) Analysis of Superplastic Deformation During Isothermal Martensitic Transformation. *Res. Mech.* 17: 241-252.
- [12] Ortin J, Planes A (1989) Thermodynamic analysis of thermal measurements in thermoelastic martensitic transformation. *Acta metall.* 36: 1873-1889.
- [13] J. van Humbeck and R. Stalmans (1998) Characteristics of shape memory alloys. Chp. 7 in Osuka K and Wayman C editors. *Shape memory materials*, Cambridge, Cambridge University Press, p. 151.
- [14] Leclercq S, Lexcelent C (1996) A general macroscopic description of the thermomechanical behavior of shape memory alloys. *J.Mech.Phys.Solids*, 44(6): 953-980.
- [15] Lexcelent C, Boubakar M L, Bouvet Ch, Calloch S (2006) About modelling the shape memory alloy behaviour based on the phase transformation surface identification under proportional loading and anisothermal conditions. *Int. J. of Sol. and Struct.* 43: 613-626.
- [16] Planes A, Macquron J L, Ortin J (1988) Energy contributions in the martensitic transformation of shape-memory alloys. *Phil. Mag. Let.* 57(6): 291-298.
- [17] Elrasasi T Y, Dobróka M M, Daróczy L, Beke D L. (2012) Effect of thermal and mechanical cycling on the elastic and dissipative energy in CuAl(11.5W%)Ni(5.0W%) shape memory alloy. *J of Alloys and Comp.* (in print)
- [18] Elrasasi T Y, Daróczy L, Beke D L (2010) Investigation of thermal and stress induced hysteresis curves in CuAl(11.5 wt%)Ni(5.0 wt%) single crystalline shape memory alloy. *Intermetallics* 18: 1137, 2010
- [19] Beke D L, El Rasasi T Y, Daróczy L (2009) On the temperature and stress dependence of transformation strain in single crystalline Cu–Al–Ni shape memory alloys. *ESOMAT Proceedings*. Available: <http://dx.doi.org/10.1051/esomat/200902002>.
- [20] Chernenko V A, L'vov V A (1996) Thermodynamics of martensitic transformations affected by hydrostatic pressure. *Phil. Mag.* A73: 999-1008.

- [21] Johari, G P, McAnanama J G, Sartor G (1996) Effect of hydrostatic pressure on the thermoelastic transformation of Ni-Ti alloy and the entropy of transformation. *Phil. Mag.* B74: 243-257.
- [22] Palánki Z, Theses, (2008) Departement Mecanique, Universite de Franche-Comte, France.
- [23] Hamilton R F, Sehitoglou H, Chumljakov Y, Maier H J (2004) Stress dependence of the hysteresis in single crystal NiTi alloys. *Acta Mater.* 52: 3383-3402.
- [24] Elrasasi T Y, Daróczy L, Beke D L (2010) On the relation between the martensite start stress and the temperature in single crystalline Cu-11.5wt%Al-5.0wt%Ni shape memory alloy. *Mat. Sci. Forum*, 659: 399-404.
- [25] Rodriguez-Aseguinolaza J, Ruiz-Larrea I, No M L, Lopez-Echarri A, San Juan J (2008) A new quantitative approach to the thermoelastic martensitic transformation: The density of elastic states. *Acta Mater.* 56: 6283-6290.
- [26] Otsuka K, Sakamoto H, Shimizu K (1979) Successive stress-induced martensitic transformations and associated transformation pseudoelasticity in Cu-Al-Ni alloys. *Acta Metall.* 27: 585-601.
- [27] Kato H, Miura S (1995) Thermodynamical analysis of the stress-induced martensitic transformation in Cu-15.0 at.% Sn alloy single crystals. *Acta metall. Mater.* 43(1): 351-360.